DLEY KNOX LIBRARY
AVAL POSTGRADUATE SCHOOL
ONTEREY, CALIFORNIA 93943-5002

NAVAL POSTGRADUATE SCHOOL
Monterey, California

THESIS

P5331

Matched Field Processing for
Underwater Source Location

by

David D. Pierce
December 1989

Thesis Advisor: C.W. Therrien
Co-Advisor J.H. Miller

Approved for public release; distribution is unlimited.

T247318

Unclassified

ecurity Classification of this page

REPORT DOCUMENTATION PAGE

a Report Security Classification Unclassified	1b Restrictive Markings
a Security Classification Authority	3 Distribution Availability of Report
b Declassification/Downgrading Schedule	Approved for public release; distribution is unlimited
Performing Organization Report Number(s)	5 Monitoring Organization Report Number(s)
a Name of Performing Organization: Naval Postgraduate School; 6b Office Symbol (*If Applicable*): 52	7a Name of Monitoring Organization: Naval Postgraduate School
c Address (*city, state, and ZIP code*): Monterey, CA 93943-5000	7b Address (*city, state, and ZIP code*): Monterey, CA 93943-5000
a Name of Funding/Sponsoring Organization; 8b Office Symbol (*If Applicable*)	9 Procurement Instrument Identification Number
c Address (*city, state, and ZIP code*)	10 Source of Funding Numbers: Program Element Number; Project No; Task No; Work Unit Accession No

1 Title (*Include Security Classification*) MATCHED FIELD PROCESSING FOR UNDERWATER SOURCE LOCATION

2 Personal Author(s) Pierce, David D.

3a Type of Report	13b Time Covered	14 Date of Report (*year, month,day*)	15 Page Count
Master's Thesis	From To	December 1989	65

6 Supplementary Notation The views expressed in this thesis are those of the author and do not reflect the official policy or position of the Department of Defense or the U.S. Government.

7 Cosati Codes			18 Subject Terms (*continue on reverse if necessary and identify by block number*)
ield	Group	Subgroup	Matched Field Processing; Underwater Source Location.

9 Abstract (*continue on reverse if necessary and identify by block number*

Matched-field Processing is a generalization of plane-wave beamforming which allows localization of an nderwater acoustic source in range and depth. Four Matched-field Processing algorithms — the Bartlett, Minimum-variance, Linear Prediction, and MUSIC methods — are compared, via numerical simulation, with egard to: 1) their resolution; 2) their performance in high-noise environments; and 3) their sensitivity to modelir rrors. The Linear Prediction method was plagued by spurious peaks for all realistic noise levels. The Bartlett, Minimum-variance, and MUSIC methods showed approximately equal sensitivity to errors in knowledge of the ound speed profile. However, the MUSIC method, which has received little attention in Matched-field rocessing applications, provided greater resolution and greater resistance to noise than either the Bartlett or Minimum-variance methods.

0 Distribution/Availability of Abstract	21 Abstract Security Classification	
[X] unclassified/unlimited [ ] same as report [ ] DTIC users	Unclassified	
2a Name of Responsible Individual: Prof. C.W. Therrien	22b Telephone (*Include Area code*): (408) 646-3347	22c Office Symbol: 62Ti

D FORM 1473, 84 MAR 83 APR edition may be used until exhausted

All other editions are obsolete

security classification of this pa

Unclassifie

Approved for public release; distribution is unlimited.

Matched Field Processing for Underwater Source Location

by

David D. Pierce
Lieutenant, United States Navy
B.S., University of Rochester, 1983

Submitted in partial fulfillment of the
requirements for the degree of

**MASTER OF SCIENCE IN ENGINEERING
ACOUSTICS**

from the

NAVAL POSTGRADUATE SCHOOL
December 1989

ABSTRACT

Matched-field Processing is a generalization of plane-wave beamforming which allows localization of an underwater acoustic source in range and depth. Four Matched-field Processing algorithms, the Bartlett, Minimum-variance, Linear Prediction, and MUSIC methods, are compared, via numerical simulation, with regard to: 1) their resolution; 2) their performance in high-noise environments; and 3) their sensitivity to modeling errors. The Linear Prediction method was plagued by spurious peaks for all realistic noise levels. The Bartlett, Minimum-variance, and MUSIC methods showed approximately equal sensitivity to errors in knowledge of the sound speed profile. However, the MUSIC method, which has received little attention in Matched-field Processing applications, provided greater resolution and greater resistance to noise than either the Bartlett or Minimum-variance methods.

DU
NA
MO
P5331
C.1

TABLE OF CONTENTS

I. INTRODUCTION 1
II. BACKGROUND 3
A. PLANE-WAVE BEAMFORMING (PWB) 3
1. Basic Idea 3
2. Signal Model 3
3. Beamforming Algorithms 3
a. Weighted-sum Beamforming 4
b. Linear Prediction. 7
c. MUSIC 8
4. Summary 10
III. MATCHED-FIELD PROCESSING (MFP) 12
A. LIMITATIONS OF PLANE-WAVE BEAMFORMING 12
1. Information obtained 12
2. Bias 12
3. Loss of gain 12
B. SIGNAL MODEL IN MFP 13
1. Introduction. 13
2. Normal mode model 14
3. Fast-field Programs (FFP) 15
4. Parabolic Equation (PE) Model 15
C. MFP ALGORITHMS 17
IV. RESULTS 18
A. EXPERIMENTAL TECHNIQUE 18
1. Numerical Simulation 18
2. Channel Characteristics 18
3. Noise modeling 18
B. RESULTS OF THE SIMULATIONS 20
1. Comparison of Ambiguity Surfaces 21
2. Sensitivity of algorithms to parameter variation 22
a. Effect of SNR changes 22
b. Effect of systematic error in SSP 23
c. Effect of random error in SSP 23
3. Summary 23
V. CONCLUSIONS AND RECOMMENDATIONS 44
LIST OF REFERENCES 45
APPENDIX— A GEOMETRIC APPROACH 47
INITIAL DISTRIBUTION LIST 60

I. INTRODUCTION

Throughout the history of submarine warfare, there has been great interest in the use of passive acoustic measurements to localize submarines. Plane-wave beamforming (PWB) has been the method of choice for determining the direction to a submerged acoustic source, from the beginning of World War II up through the present. However, PWB is inherently incapable of directly determining the range and depth of a target (although there are indirect means of determining range by observing target direction as a function of time). Because knowledge of range and depth is so vital in military applications, there has been considerable interest in developing techniques for direct determination of these parameters. One such technique, which has attracted considerable attention in recent years, is a generalization of PWB known as Matched-Field Processing (MFP) (see, for example, Baggeroer, *et al.*, 1988, and Fizell, 1987).

Because of the similarity between PWB and MFP, many of the techniques used in PWB may be generalized for use in MFP. Two PWB methods—the Bartlett and Minimum-Variance methods—have been studied extensively in the context of MFP (Baggeroer *et al.*, 1988). Two other algorithms—Linear Prediction and MUSIC—which have gained great popularity in the fields of time-series analysis and array processing (see, *e.g.*, Kay, 1988, and Schmidt, 1981), have received little attention from MFP

DU
NA
MO

researchers. The objective of the research is to compare the performance of Bartlett, Linear Prediction, Minimum Variance and MUSIC MFP algorithms with regard to:

- Resolution (*i.e.,* the ability to resolve two or more targets which are close to each other);
- Behavior when signal-to-noise ratio (SNR) is low;
- Sensitivity to inexact knowledge of the sound speed profile.

Chapter II gives an introduction to the theory of PWB, and discusses the theoretical basis for the most popular algorithms. Chapter III discusses the limitations of PWB, gives an introduction to the modeling of underwater sound propagation, and describes the theoretical framework of MFP. Chapter IV discusses the method used for performing numerical simulation, as well as the results of the simulation. Chapter V gives the conclusions reached from the research and proposes areas for further investigation.

II. BACKGROUND

A. PLANE-WAVE BEAMFORMING (PWB)

1. Basic Idea

One of the most fundamental parameters of interest in military applications is the Direction-of-Arrival (DOA) corresponding to a target of interest. Plane-wave beamforming (PWB) is the most commonly used technique for estimating an emitter's DOA, and is used in all modern military radar and sonar systems. Essentially, the technique involves predicting, based on realistic assumptions about the characteristics of the received signal, what (electromagnetic or acoustic) field the receiving array would observe as a function of actual target DOA. The DOA for which the *predicted* received signal "most closely matches" (in some statistical sense) the *actual* received signal is chosen as the estimated DOA. In the sequel, we will discuss PWB in the context of underwater sonar.

2. Signal Model

As is the case with most signal processing algorithms, PWB makes certain assumptions about the signals being processed. It assumes, in particular, that the pressure field in the underwater channel is a plane wave (*i.e.,* the surfaces of constant phase are planar). It frequently also assumes (as we do here) that the signals are narrow-band.

3. Beamforming Algorithms

Numerous signal processing algorithms have been studied in the context of PWB. Actually, some of these algorithms (including Linear

Prediction and MUSIC) do not perform "beamforming" in the strict sense of the word, so this nomenclature is somewhat imprecise. Many are fairly obvious generalizations of techniques used for estimating the spectra of time series. In PWB, as in time-series analysis, certain assumptions are made about the nature of the noise present at the receiving array. Each algorithm then gives an estimate of the direction-of-arrival of the incident signal. Each estimate is "optimum" in some sense, provided that the underlying assumptions are valid. In the following, we will briefly review four of the more popular PWB algorithms.

The concept of a *replica field* is one that arises often in PWB and MFP. To understand this concept, consider an arbitrary receiving array of N elements. We may represent the signal as an N-dimensional, time-varying, complex vector whose components are the signals at the individual array elements. The components are complex because we will work with the pre-envelope of the signal rather than the signal itself. The replica field $\mathbf{a}(\theta)$ is defined to be the normalized, noise-free, pressure field vector that is expected at the array given that the source is at the angle θ. For the case of narrowband plane waves, $\mathbf{a}(\theta)$ may be expressed as

$$\mathbf{a}(\theta) = \left[1 \;\; e^{-j\omega\tau_1} \ldots e^{-j\omega\tau_{N-1}}\right]^T,$$

where τ_i represents the time delay seen by the incoming plane wave between sensor i and sensor 0, and T denotes matrix transpose.

a. Weighted-sum Beamforming (Van Veen, 1988)

This technique is entirely analogous to the use of Finite Impulse Response (FIR) filters in time-series analysis. The output $b(t)$ of the

beamformer is a linear combination of the signals received at the individual elements of the array,

$$b(t) = \mathbf{w}^H(\theta)\mathbf{p}(t)\,,$$

where $\mathbf{p}$ is the vector of (noisy) time-varying pressures at the individual sensors, and $\mathbf{w}$ is a vector of weights (H denotes hermitian transpose). The components of $\mathbf{w}$ are chosen to satisfy a statistical constraint which is appropriate for the given situation. The vector $\mathbf{w}$ will, in general, depend on the assumed target direction θ. The expected value B of the output power of the beamformer is given by

$$B = \mathbf{w}^H(\theta)\,\mathbf{R}_\mathbf{p}\,\mathbf{w}(\theta)\,,$$

where $\mathbf{R}_\mathbf{p}$ is the signal-plus-noise covariance matrix. The value of θ for which this expression is maximized is taken as the estimated DOA.

Bartlett Method. In this method, the beamformer weights are the (normalized) complex conjugates of the signals expected at each element (*i.e.*, $\mathbf{w} = \mathbf{a}(\theta)$). When the noise is spatially homogeneous, the output of this beamformer has the highest possible SNR of any weighted-sum beamformer. The expected value of the output (signal plus noise) power is given by

$$B(\theta) = \mathbf{a}^H(\theta)\,\mathbf{R}_\mathbf{p}\,\mathbf{a}(\theta)\,. \qquad (2.1)$$

This is essentially the algorithm used in all modern military direction-finding systems. Experience has shown its resolution to be more than adequate for many applications. It has also proven quite robust with respect

DJT
NAV
MON

to modeling errors. However, at low frequencies (such as those of current interest in the area of passive sonar), its resolution is unacceptably low (see, *e.g.*, Barabell, *et al.*, 1984, p. 17). For this reason, the three "high-resolution" methods discussed in the sequel (as well as others not discussed here) have attracted great interest in recent years.

Minimum-Variance (MV) Method. This method (Capon, 1969; Kay, 1988), often somewhat misleadingly referred to as the "maximum likelihood" method, chooses the beamformer weights to minimize the beamformer output power, subject to the constraint of unity gain for signals from the desired look direction. The weights are given by

$$\mathbf{w}(\theta) = \frac{\mathbf{R}_p^{-1}\mathbf{a}(\theta)}{\mathbf{a}^H(\theta)\,\mathbf{R}_p^{-1}\mathbf{a}(\theta)}, \tag{2.2}$$

and the expectation value of the output power is

$$B(\theta) = \frac{1}{\mathbf{a}^H(\theta)\,\mathbf{R}_p^{-1}\mathbf{a}(\theta)}. \tag{2.3}$$

The resolution of this algorithm is significantly higher than that of the Bartlett method, but lower than that of the Linear Prediction or MUSIC algorithms. In addition, it is better able to deal with spatially correlated noise and interfering sources than the other three methods, all of which assume spatially white noise.*

---

* Of course, if the covariance matrix of the noise is known or can be accurately estimated, the noise may be prewhitened so as to negate this advantage.

b. Linear Prediction.

This method is a generalization of the autoregressive (AR) spectral estimate (Kay, 1988). It was first studied in the context of matched-field processing by Klemm (1981) who called it the Approximate Orthogonal Projection (AOP) technique. In this method, the signal present at the Nth array element can be estimated as a linear combination of the signals present at all the other elements:

$$p_N = \sum_{k=1}^{N-1} b_k p_{N-k} \ .$$

As is well known, the AR model coefficients b_k which give the minimum mean-square error can be found from the normal equations

$$\mathbf{R}_p \mathbf{b} = \sigma^2 \begin{bmatrix} 1 \\ 0 \\ \vdots \\ 0 \end{bmatrix} .$$

In analogy with the AR spectral estimate, the DOA estimator is then defined as

$$B(\theta) = \frac{\sigma^2}{\left|\mathbf{b}^H \mathbf{a}(\theta)\right|^2} . \tag{2.4}$$

This estimator has high resolution, but spurious peaks are more of a problem than for other estimators (Kay, 1988, p. 420). The presence of spurious peaks is fundamentally due to the fact that the signal model

assumed by the Linear Prediction method is a poor representation of the physics of the DOA estimation problem (Roy, 1987, p. 33).

c. MUSIC

The technique known as MUSIC (short for MUltiple SIgnal Classification) (Schmidt, 1981) is rather involved mathematically, to the extent that it cannot be discussed fully in this limited survey. In the sequel, we give only a very brief overview. The reader is referred to the appendix for more details.

For simplicity, consider the case of two narrowband sources at DOA's θ_1 and θ_2 whose signals impinge upon a three-element array. This receiving array consists of elements with arbitrary location and arbitrary response patterns. The vector whose components are the (time-varying) pressures at each receiving element sweeps out (over time) a two-dimensional surface, shown by the gray plane in Figure 2.1. This surface is known as the *signal subspace* and its dimension is equal to the number of sources present. Even in the presence of observation noise, the signal subspace can be accurately estimated using an eigendecomposition of the signal-plus-noise covariance matrix. The response of the array as a function of DOA (*i.e.*, the mapping from DOA space to signal vector space) can be expressed geometrically as an *array manifold* (see Figure 2.1). The intersections of the array manifold with the signal subspace are those response vectors which correspond to the actual source DOA's. If one assumes that the mapping from DOA space to signal vector space is one-to-one, these array response vectors can be used to find the source DOA's.

The method outlined in the previous paragraph can be used to determine the source DOA's *exactly* when the *exact* signal-plus-noise covariance matrix is known. Since such perfect knowledge never occurs in practice, the covariance matrix must be *estimated* from the measured data. Due to estimation errors, it may turn out that the estimated signal subspace does not intersect the array manifold. The MUSIC algorithm deals with this problem by introducing the concept of the *noise subspace* (see Figure 2.1), which is the orthogonal complement of the signal subspace. It can be shown that the eigenvectors of $\mathbf{R}_p$ corresponding to the smallest eigenvalues span the noise subspace. When there are no estimation errors, the array response vectors corresponding to the correct source DOA's are those whose projection onto the noise subspace is zero. If $\mathbf{E}_N$ is defined to be any matrix whose columns form an orthonormal basis for the noise subspace, then the projection $\mathbf{v}$ of an array response vector onto the noise subspace is given by

$$\mathbf{v} = \mathbf{E}_N^H \mathbf{a}(\theta). \tag{2.5}$$

When estimation errors are present, we take the estimated DOA's to be those which minimize the length of this projection vector. Alternatively, we may form the pseudo-spectrum

$$B(\theta) = \frac{1}{\mathbf{a}^H(\theta)\mathbf{E}_N\mathbf{E}_N^H\mathbf{a}(\theta)}. \tag{2.6}$$

The values at which the peaks of this function occur are taken as the estimates of the source DOA's.

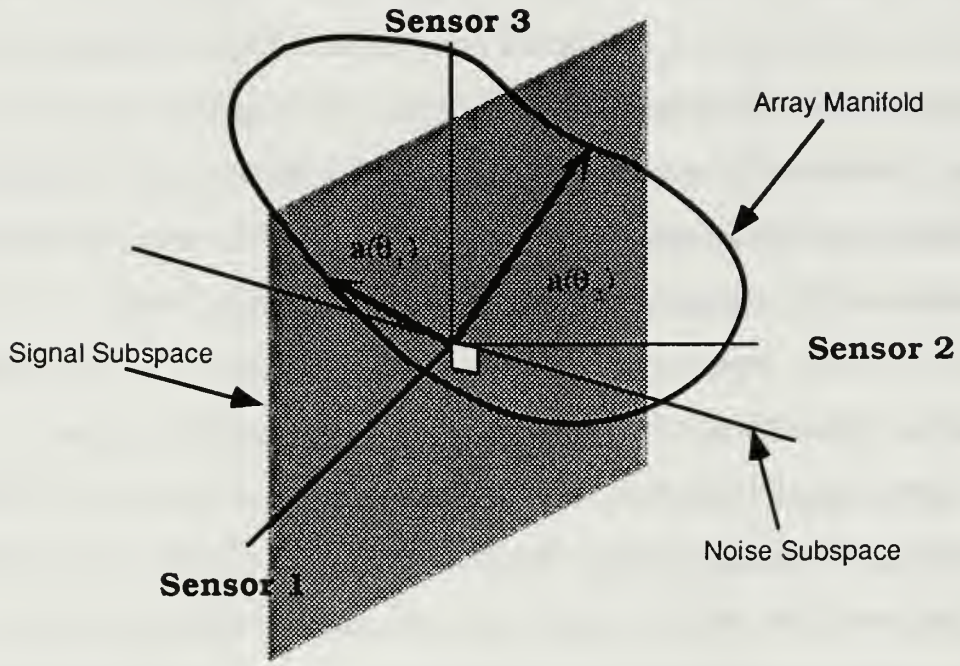

Figure 2.1: DOA Estimation (2 emitters)

The MUSIC algorithm has a higher resolution (except when the number of available time snapshots is very low), a lower false alarm rate, and a lower estimate variance than the other high-resolution methods discussed here (Barabell, *et al.*, 1984). It does, however, require more computational effort.

4. Summary

We have outlined the theoretical basis for four of the most popular algorithms used for time-series analysis and PWB—the Bartlett, Minimum-variance, Linear Prediction, and MUSIC methods. Again, despite the large amount of attention the Linear Prediction and MUSIC

algorithms have received in time-series analysis and PWB, they have received little attention in MFP. The strengths of these two algorithms in PWB provide a significant incentive to apply them to MFP, which we do in the following chapters.

III. MATCHED-FIELD PROCESSING (MFP)

A. LIMITATIONS OF PLANE-WAVE BEAMFORMING

In this section, we discuss the limitations inherent in PWB to provide motivation for the study of MFP.

1. Information obtained

Because of the assumption that the received signal is a plane wave, the only degree of freedom in the replica fields is DOA. Therefore, PWB is inherently incapable of providing any information besides DOA. In particular, PWB gives no range information, which in military applications is of vital interest.

2. Bias

Since the speed of wave propagation is a function of position, the sound "rays" (*i.e.,* paths normal to the surfaces of constant phase) will be curved. Consequently, the DOA estimate obtained from PWB, will, in general, be different from the actual direction of the emitter. In many situations, the ocean may be considered to be horizontally stratified (*i.e.,* speed of propagation is a function primarily of depth). In such situations, although there may be significant error in the target elevation estimate, there may be little error in the azimuth estimate.

3. Loss of gain

We have noted earlier that the Bartlett beamformer results in the highest output SNR, provided that the noise is spatially homogeneous. Essentially, this feature is due to the fact that the signal is averaged

coherently while the noise is averaged *incoherently*. In an underwater channel, however, due to the presence of wavefront curvature and multipath propagation, the signals from the array elements are in fact *not* coherently averaged by the Bartlett beamformer. A similar phenomenon occurs with the other methods, in that their ability to distinguish between signal and noise is reduced because of incorrect modeling of the signal. Consequently, the performance of all of the above methods will be poorer in a realistic underwater environment than it would be in an environment where the incoming signals are actually plane waves.

B. SIGNAL MODEL IN MFP

1. Introduction.

Whereas in DOA estimation the received signals are assumed to be plane waves, in MFP the pressure field in the channel is assumed to satisfy the Helmholtz equation

$$\frac{1}{r}\frac{\partial}{\partial r}\left(r\frac{\partial p}{\partial r}\right)+\frac{\partial^2 p}{\partial z^2}+k^2 p=0. \tag{3.1}$$

which is the differential equation satisfied by the field due to a harmonic source in the linear acoustics approximation. The signal models (to be discussed in the sequel) used in MFP essentially consist of different methods of numerically approximating the solution to (3.1).

2. Normal mode model

In a channel where all properties (sound speed, water depth, bottom type, etc.) are independent of horizontal range, it is well known (Clay and Medwin, 1977) that the pressure field at a horizontal range r (relative to a point emitter) sufficiently far away from the source and at a depth z may be expanded in terms of normal modes. The normal mode expansion is given by

$$p(r,z) = \sum_{m=1}^{\infty} \frac{A}{\sqrt{k_m r}} U_m(z) U_m(z_0)\, e^{-jk_m r} + n(z)\,, \tag{3.2}$$

where the k_m are the horizontal wavenumbers, z_0 is the source depth, n is additive noise, and A is a (complex) constant which depends on the power output of the source. The U_m are eigenfunctions of the ordinary differential equation

$$\frac{d^2 U_m}{dz^2} + \left[\frac{\omega^2}{c^2(z)} - k_m^2\right] U_m = 0\,.$$

Although the sum in (3.2) is over values of m from zero to infinity, all modes for which m is greater than some integer M ("evanescent modes") are sufficiently attenuated that they can be ignored at the ranges of interest. For simplicity, we neglect absorption in this formulation. It should be noted that the expansion (3.2) is only approximate, in that it gives only the discrete set of solutions to the Helmholtz equation (3.1). This fact does not present a problem, however, because the contribution to the pressure field from the continuous set of solutions is negligible at the ranges of interest in MFP.

Several numerical algorithms exist (*e.g.*, Porter, 1985) for implementing this solution (3.2) on a computer; the best of these use an FFT-type algorithm to solve for the pressure at all ranges simultaneously. Most, but not all, normal mode algorithms are limited to situations which are range-independent or at least nearly so, so that no mode coupling occurs.

3. Fast-field Programs (FFP) (Schmidt, 1985)

These programs compute the pressure field by means of a numerical approximation to the Green's function solution of the Helmholtz equation (3.1). As in some of the normal mode methods, an FFT is used to give the field at all ranges simultaneously. Unlike the normal mode methods, however, FFP's compute the continuous set as well as the discrete set of solutions to the Helmholtz equation (3.1). For this reason, FFP's are known as *full-wave* propagation models.

4. Parabolic Equation (PE) Model

The Helmholtz equation (3.1) is an elliptic partial differential equation (PDE), and therefore requires knowledge of boundary conditions for its solution. A numerical method would simultaneously find the pressure at each point on a mesh inside the boundary by solving a huge system of simultaneous linear equations. Such a technique would be virtually useless in practice because boundary conditions are never known completely and computational expense would be excessive. However, if it is

assumed that the angle within which the source radiates is small (less than about 20°)*, we obtain the PDE

$$\frac{\partial^2 \zeta}{\partial z^2} + 2jk_0 \frac{\partial \zeta}{\partial r} + (k^2 - k_0^2)\zeta = 0 ,$$

where we define

$$p(r,z) = H_0^{(1)}(k_0 r)\, \zeta(r,z) .$$

$H_0^{(1)}$ is the zero-order Hankel function of the first kind and k_0 is a reference wavenumber. This is a parabolic PDE, which does not require complete knowledge of boundary conditions. The numerical solution at each horizontal range step is completely determined by the solution at the previous step. Thus, once we have determined the solution at zero range, we may "march out" the solution to any desired range. In practice, the solution is determined at all ranges simultaneously via an FFT-type algorithm.

The advantage of the PE method over normal mode methods is that it may be used with a highly range-dependent channel. Owing to the small-angle assumption, it is somewhat less accurate than normal mode methods. This inaccuracy may be partially overcome by the use of higher order approximations to the Helmholtz equation (3.1), but at higher computational expense. Like the FFP, the PE method is a full-wave method. For a summary of this technique, see Coppens (1982).

---

* Such an assumption is not unrealistic, since any sound leaving the source at steeper angles will have numerous interactions with the surface and bottom and will be largely attenuated by the time it reaches the (distant) receivers.

C. MFP ALGORITHMS

All algorithms discussed in Chapter II in the context of PWB may be generalized in a more-or-less straightforward way to MFP, and are optimal in precisely the same sense in MFP as in PWB. In PWB, the replica fields $\mathbf{a}(\theta)$ are the array response vectors for a plane wave arriving from azimuth θ. In MFP, the replica fields $\mathbf{a}(r, z)$ are the array response vectors for a source at range r and depth z, as predicted by some propagation model. Then, by analogy with equation (2.1), the power output of the Bartlett MFP beamformer (the expressions for the other algorithms are analogous) is given by

$$B(r,z) = \mathbf{a}^H(r,z)\,\mathbf{R}_p\,\mathbf{a}(r,z)\,.$$

A plot of B as a function of r and z is known as an *ambiguity surface*. The location of the peak of this surface is taken to be the estimate of the source location.

IV. RESULTS

A. EXPERIMENTAL TECHNIQUE

1. Numerical Simulation

The performance of all algorithms was simulated numerically via Pro-MATLAB on either a Sun 4/110 or a DEC VAX 11/785. The signal processing algorithms were written in the MATLAB programming language. The Navy standard Parabolic Equation (PE) model was chosen for all simulations because of its availability at the Naval Postgraduate School. The PE model is written in FORTRAN but called directly from MATLAB.

2. Channel Characteristics

A fairly typical North Atlantic deep-water channel was chosen for our simulations. The channel characteristics are as listed in Table 4.1, and the sound speed profile is shown in Figure 4.1. For simplicity, effects such as surface roughness, bottom propagation, and volume attenuation were ignored. Obviously, a great deal of realism is sacrificed by ignoring these effects. However, it is believed that a great deal of insight into the relative merits of the various MFP algorithms can be gained in spite of this fact.

3. Noise modeling

One of the features of the underwater acoustic signal processing problem that distinguishes it from the radar problem is the nature of the noise environment. In the radar problem, it is usually reasonable to assume that the noise is spatially uncorrelated. In the underwater acoustic

TABLE 4.1: CHANNEL CHARACTERISTICS

Channel Depth	4000 m
Source depth	125 m
Number of receivers	10
Receiver depths	$50 + 30l$ m, l=0,1,...9
Source frequency	50 Hz
Horizontal range to source	6.03 km or 9.03 km
Surface characteristics	Smooth, pressure-release
Bottom characteristics	Smooth, fully-absorbing

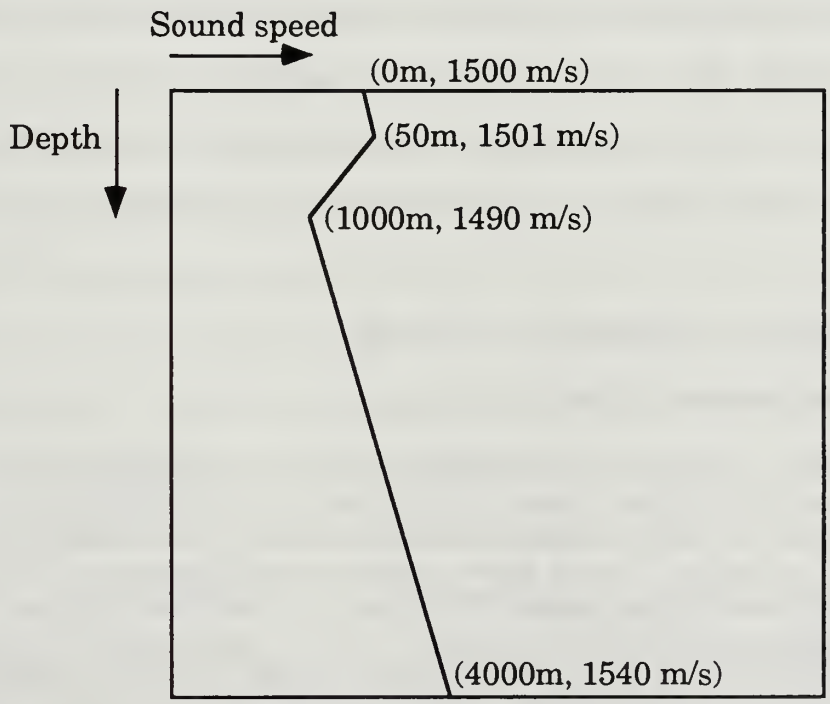

Figure 4.1: Sound speed profile

problem, the noise is quite similar to that of the signal of interest. Obviously, any serious study must take into account a realistic noise environment by simulating the noise via the same acoustic propagation model used to simulate the signal. Unfortunately, due to computational constraints, it was not possible to simulate the noise in this manner in our research. For simplicity, temporally white noise having the spatial covariance

$$\mathbf{R}_n = \begin{bmatrix} 1 & \rho & \rho^2 & \cdots & \rho^{N-1} \\ \rho & 1 & \rho & & \vdots \\ \rho^2 & \rho & 1 & \ddots & \\ \vdots & & \ddots & \ddots & \rho \\ \rho^{N-1} & \cdots & & \rho & 1 \end{bmatrix}$$

was modeled, where ρ is known as the noise correlation parameter. Although not physically realistic, this one-parameter model does make it easy to quantify the effect of the noise spatial correlation on the MFP algorithms. It is expected that the behavior of the algorithms in more realistic noise environments will be qualitatively similar to our results.

B. RESULTS OF THE SIMULATIONS

The results consist of the following:

- Qualitative analysis of ambiguity surfaces produced by the Bartlett, Minimum-Variance, Linear Prediction, and MUSIC methods. The motivation for this analysis is to compare the resolution (*i.e.,* the ability to resolve two or more closely-spaced targets) of the methods. Although we did not actually test any of the algorithms in situations containing more than one target, it seems reasonable to assume that algorithms which produce ambiguity surfaces with sharp peaks and low sidelobes will be better able to resolve closely-spaced targets than algorithms with broad peaks and high sidelobes.

- Comparison of the sensitivity of the range and depth estimates to:
  1) changes in SNR and noise correlation; and
  2) inexact knowledge of the sound speed profile.

It is recognized that, because a wide variety of environmental conditions is possible in an underwater channel, one cannot draw precise *quantitative* conclusions about the performance of the algorithms under consideration from the limited results presented here. Nevertheless, we expect that the *qualitative* conclusions reached herein will be valid in general. Obviously, more detailed theoretical and experimental studies will be required to verify this conjecture.

1. Comparison of Ambiguity Surfaces

Figures 4.2 through 4.13 show the ambiguity surfaces for the four algorithms for the following situations: 1) SNR=0 dB, ρ=0; 2) SNR=+20 dB, ρ=0; 3) SNR=+10 dB, ρ=0.5. For these sets of simulated conditions, the Linear Prediction method is plagued by spurious peaks and is incapable of producing a reliable estimate of the source location. In contrast, the Bartlett, Minimum-Variance, and MUSIC methods exhibit peaks at roughly the correct source location (range=9.03 km, depth=125 m). Despite the fact that they give roughly the same source location estimates, these three methods have very different ambiguity surfaces. The Bartlett method exhibits an extremely broad peak at roughly the correct source location. The ambiguity surface shows little dependence on SNR for the situations simulated. At high SNR, the Minimum-variance method shows peaks which are sharper than those of the Bartlett method. As SNR drops, the peak broadens and sidelobe levels increase. The MUSIC method produces the sharpest peaks for all simulations. The broadening of the peak and the

increase in sidelobe levels with decreasing SNR are less pronounced than for the Minimum-Variance method.

Other sets of conditions (for which the algorithms exhibited the same qualitative behavior) were also simulated, but the results are not presented here. It should be noted that, in some of these runs, the difference in resolution between the Minimum-variance and MUSIC methods was not so pronounced as in the cases presented here.

2. Sensitivity of algorithms to parameter variation

a. Effect of SNR changes

Figures 4.14 through 4.17 illustrate the dependence of the range and depth estimates upon SNR, for both spatially white and spatially correlated noise. The Linear Prediction method is plagued by the presence of spurious peaks for all values of SNR and noise correlation simulated. For the case of correlated noise, the Bartlett and MUSIC methods suffer significant performance degradation when compared to the case of spatially white noise, while there is no noticeable change in the performance of the Minimum-Variance method. This fact is to be expected, since the first two methods assume spatially white noise, whereas the third does not. For the case of spatially white noise with SNR above about –8 dB, both the Bartlett and MUSIC methods give estimates which are within 1000 m and 30 m of the true values for range and depth, respectively. The Minimum-Variance method requires a SNR of about –6 dB to provide the same performance.

b. Effect of systematic error in SSP

None of the methods shows significant sensitivity to systematic (depth-independent) sound speed errors between –10 and +10 m/sec. The results for one typical set of simulation conditions are shown in Figures 4.18 and 4.19.

c. Effect of random error in SSP (Figures 4.20 through 4.25)

The Bartlett, Minimum-Variance, and MUSIC methods exhibit approximately the same sensitivity to random errors in the SSP, giving range and depth estimates accurate to within 1000 m and 50 m, respectively, (for SNR=+10 dB and spatially white noise) when the standard deviation of the errors is less than about 2 m/s. These algorithms show higher sensitivity for lower SNR and for spatially correlated noise. The Linear Prediction method shows extreme sensitivity to errors in the SSP in all simulated conditions, again due to the presence of spurious peaks in the ambiguity function.

3. Summary

The resolution of the various methods, as qualitatively determined by evaluating the ambiguity surfaces for peak sharpness and sidelobe level, is almost entirely analogous to that observed when these algorithms are applied to PWB (see, *e.g.*, Roy, 1987, pp. 51–55). The Bartlett method exhibits a peak which, although it is at the correct range and depth, is too broad to be of practical use for the frequency and number of array elements assumed here. It also exhibits high sidelobe levels. The Minimum-variance method exhibits a sharper peak and lower sidelobes than the Bartlett method. The MUSIC method exhibits the sharpest peak and lowest sidelobes of any of the

methods. The Linear Prediction method, while it exhibits peaks of roughly the same sharpness as MUSIC, is also plagued by spurious peaks which are often higher than the true peak. It required a much higher SNR than was simulated here in order to give reliable source location estimates.

In general, there was little difference between the Bartlett, Minimum-variance, and MUSIC methods with regard to the sensitivity of their location estimates to increased noise level or to errors in knowledge of the sound speed. The only exception to this generalization is that the Minimum-variance method could tolerate lower SNR than the other algorithms when the noise was spatially correlated. This area bears further study, but it seems likely that the noise covariance could be measured with sufficient accuracy to allow prewhitening of the noise. It is expected that such a technique would significantly improve the robustness of the Bartlett and MUSIC methods with respect to high levels of spatially correlated noise.

(This page intentionally left blank)

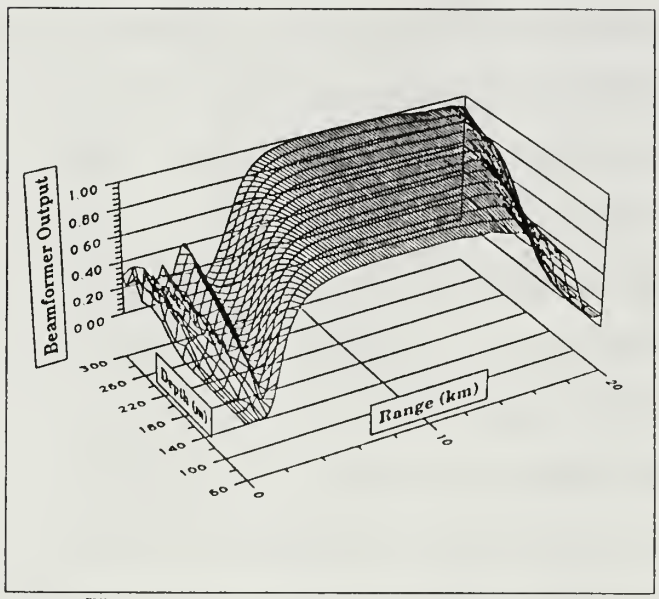

Figure 4.2: Bartlett, SNR=0 dB, ρ=0

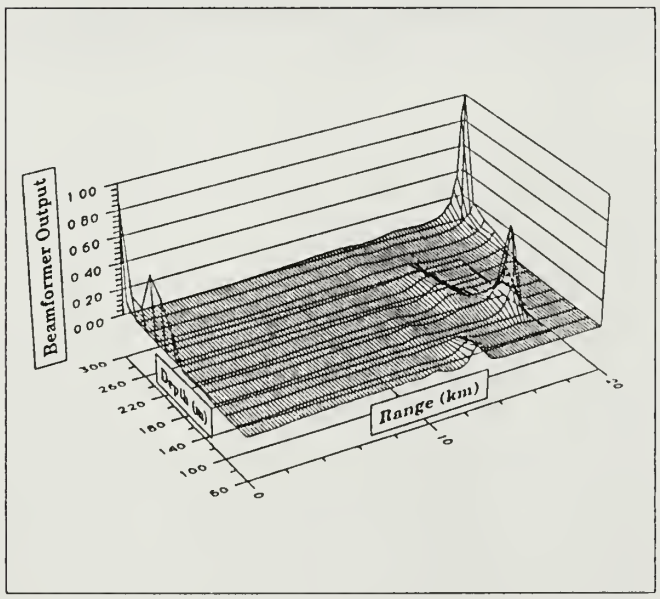

Figure 4.3: Linear Prediction, SNR=0 dB, ρ=0

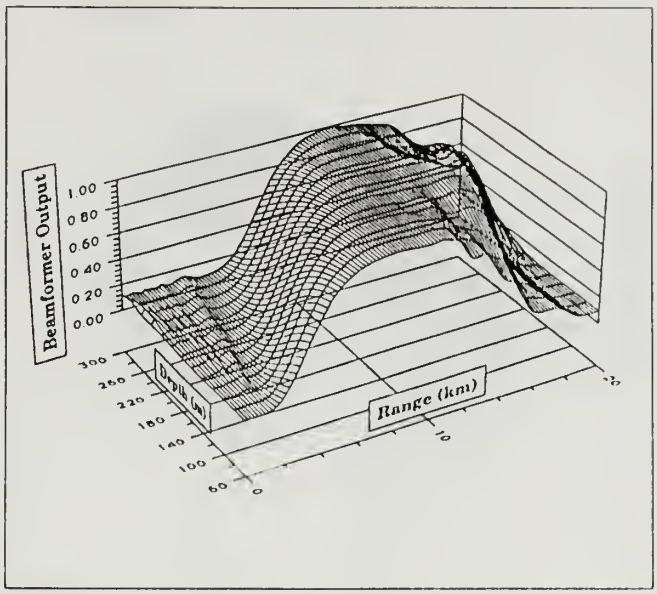

Figure 4.4: Minimum variance, SNR=0, ρ=0

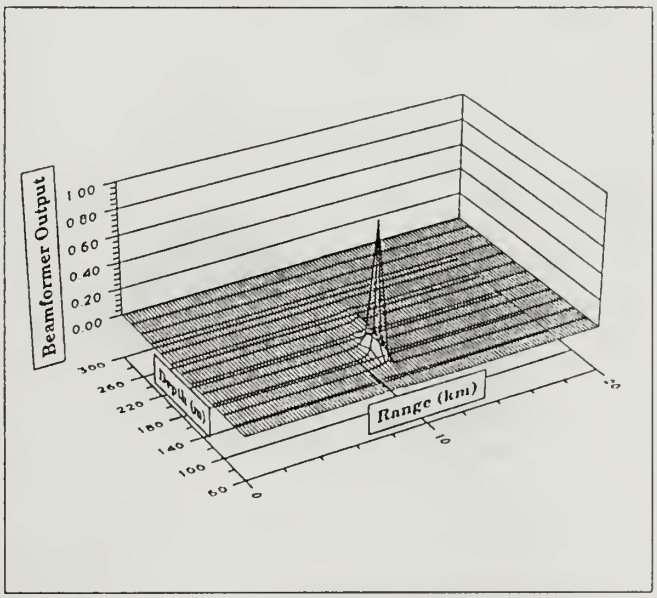

Figure 4.5: MUSIC, SNR=0 dB, ρ=0

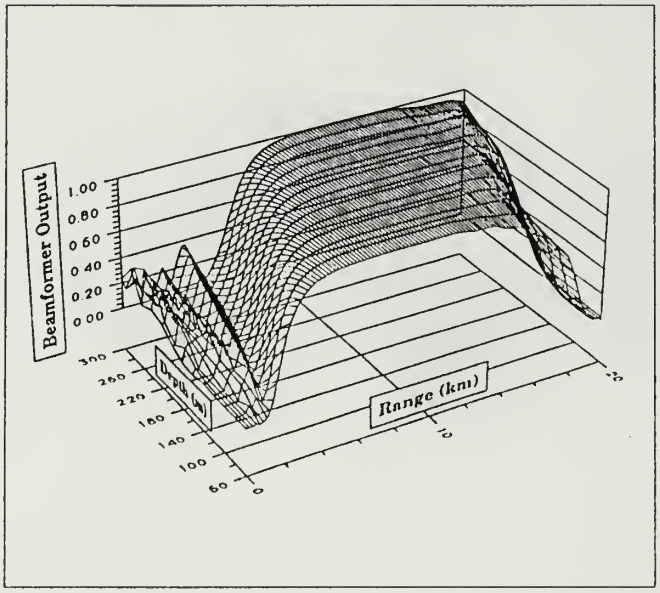

Figure 4.6: Bartlett, SNR=+10 dB, ρ=0.5

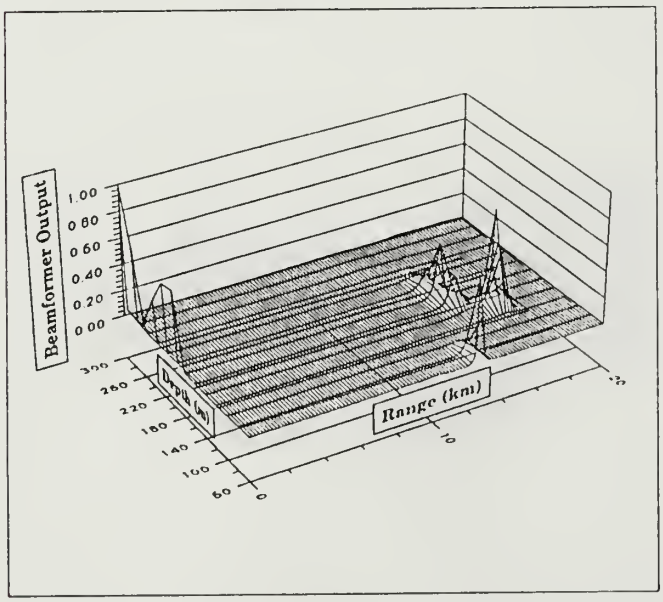

Figure 4.7: Linear prediction, SNR=+10 dB, ρ=0.5

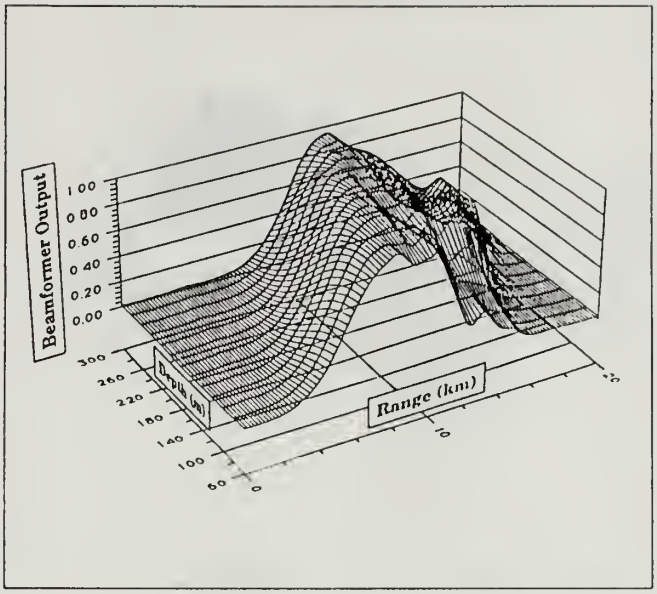

Figure 4.8: Minimum variance, SNR=+10 dB, ρ=0.5

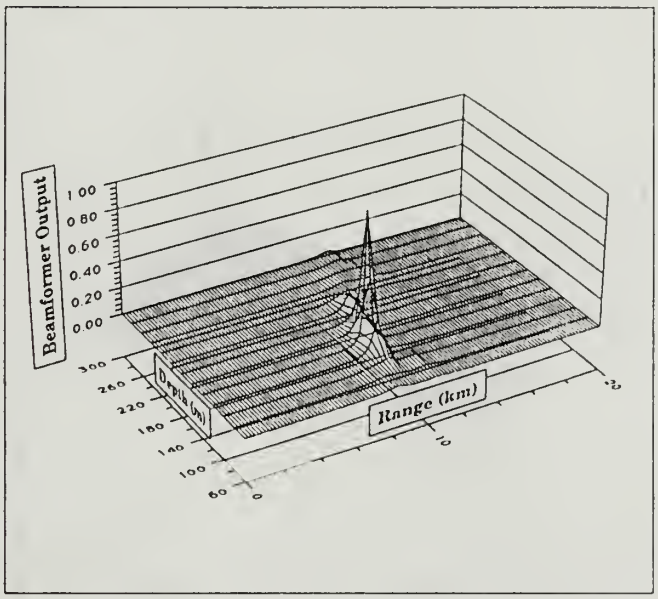

Figure 4.9: MUSIC, SNR=+10, ρ=0.5

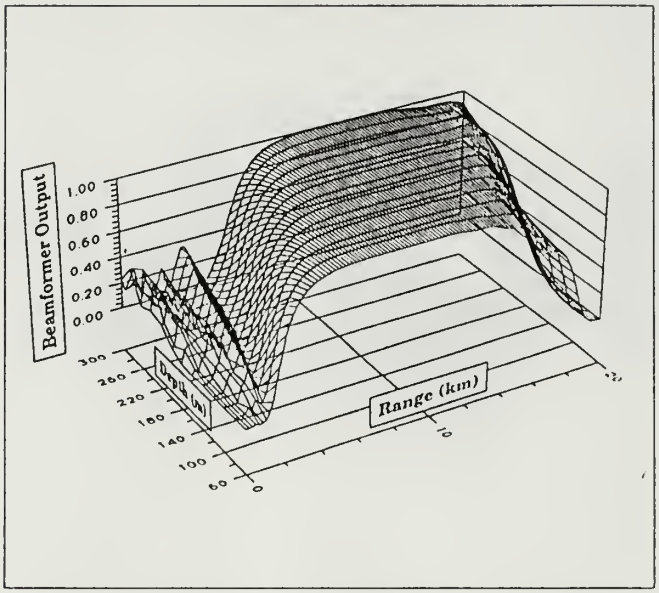

Figure 4.10: Bartlett, SNR=+20 dB, ρ=0

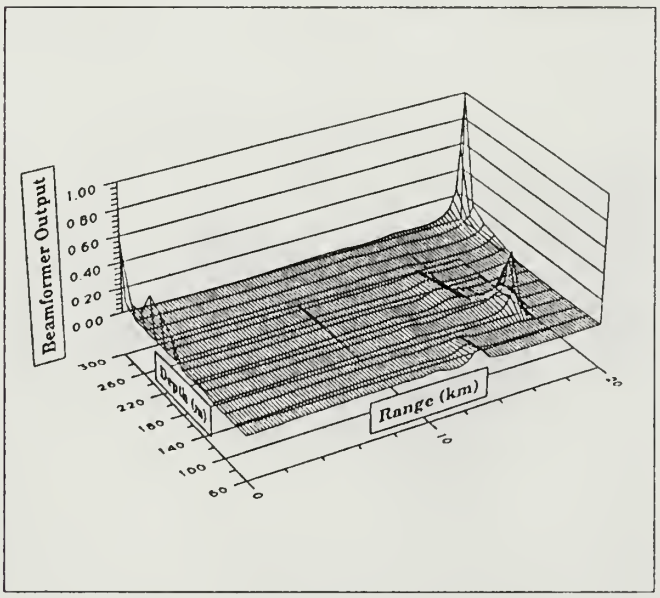

Figure 4.11: Linear Prediction, SNR=+20 dB, ρ=0

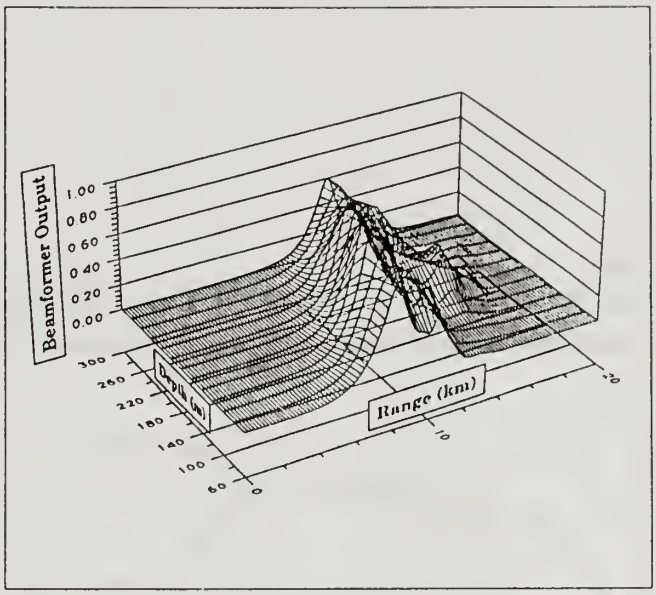

Figure 4.12: Minimum variance, SNR=+20 dB, ρ=0

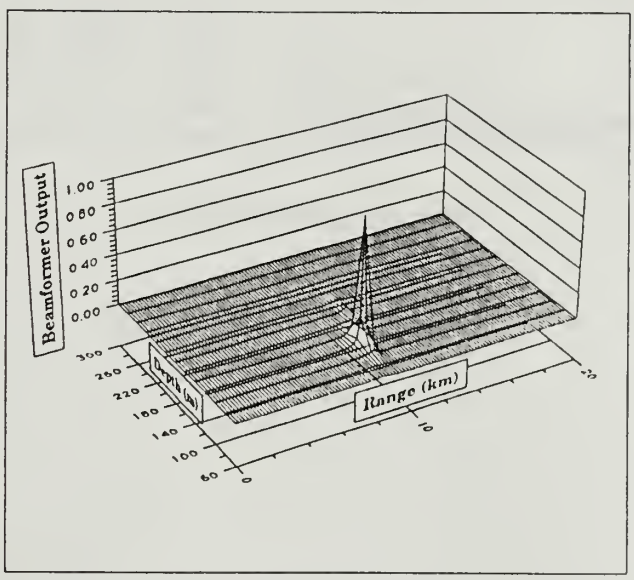

Figure 4.13: MUSIC, SNR=+20 dB, ρ=0

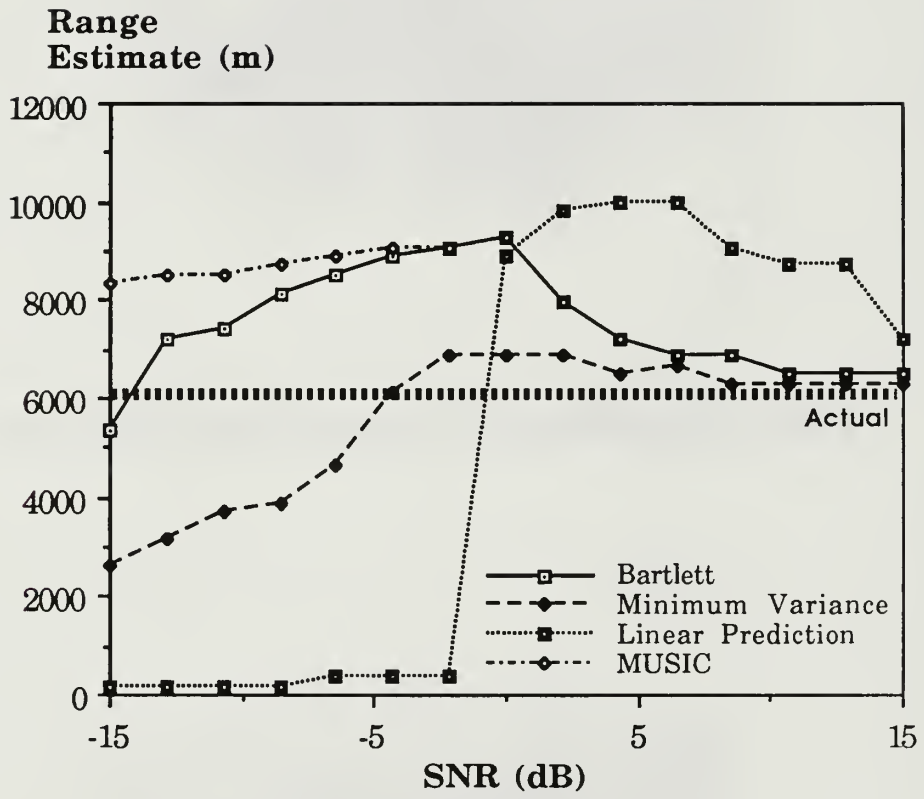

Figure 4.14: Sensitivity to SNR changes (no error in SSP, ρ=0.5)

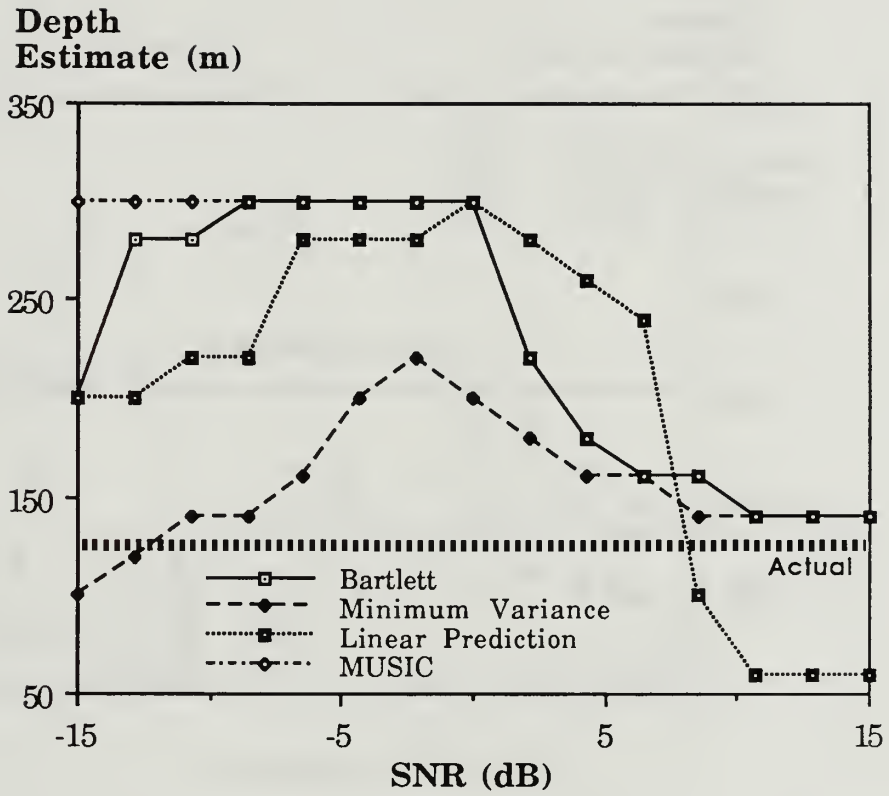

Figure 4.15: Sensitivity to SNR changes (no error in SSP, ρ=0.5)

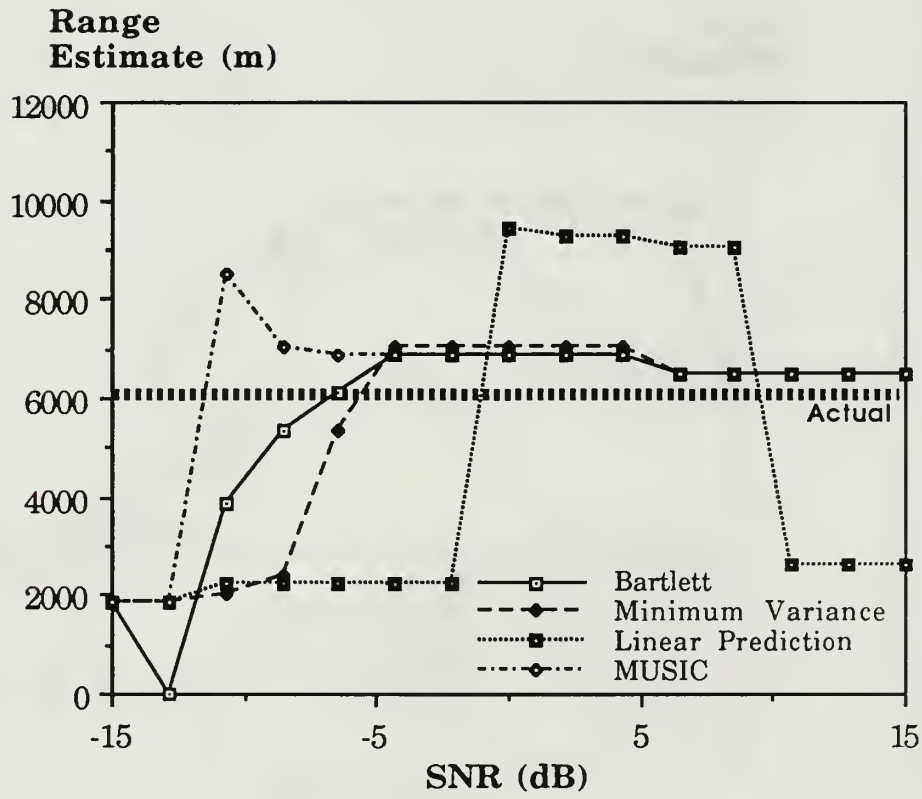

Figure 4.16: Sensitivity to SNR changes (no error in SSP, ρ=0)

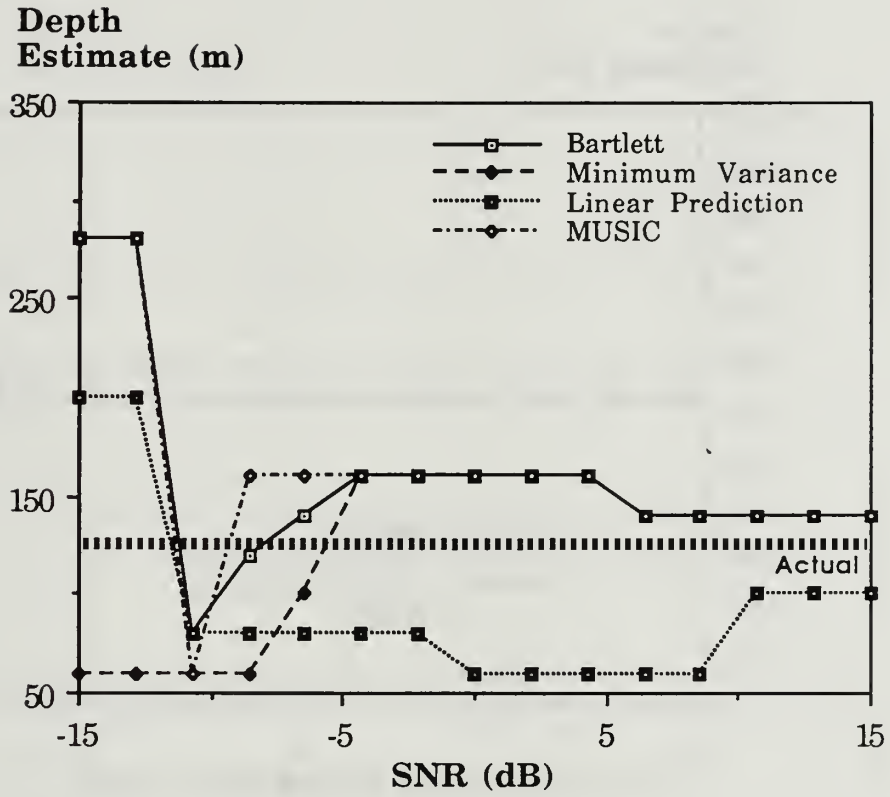

Figure 4.17: Sensitivity to SNR changes (no error in SSP, ρ=0)

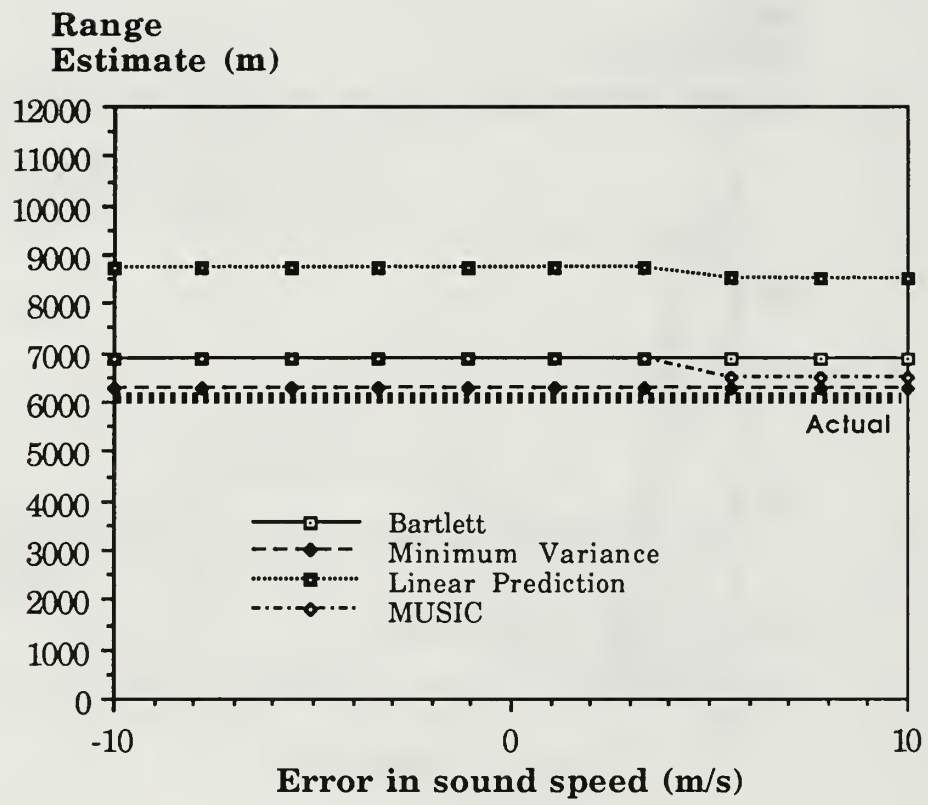

Figure 4.18: Sensitivity to systematic error in SSP (SNR=+10dB, ρ=0.5)

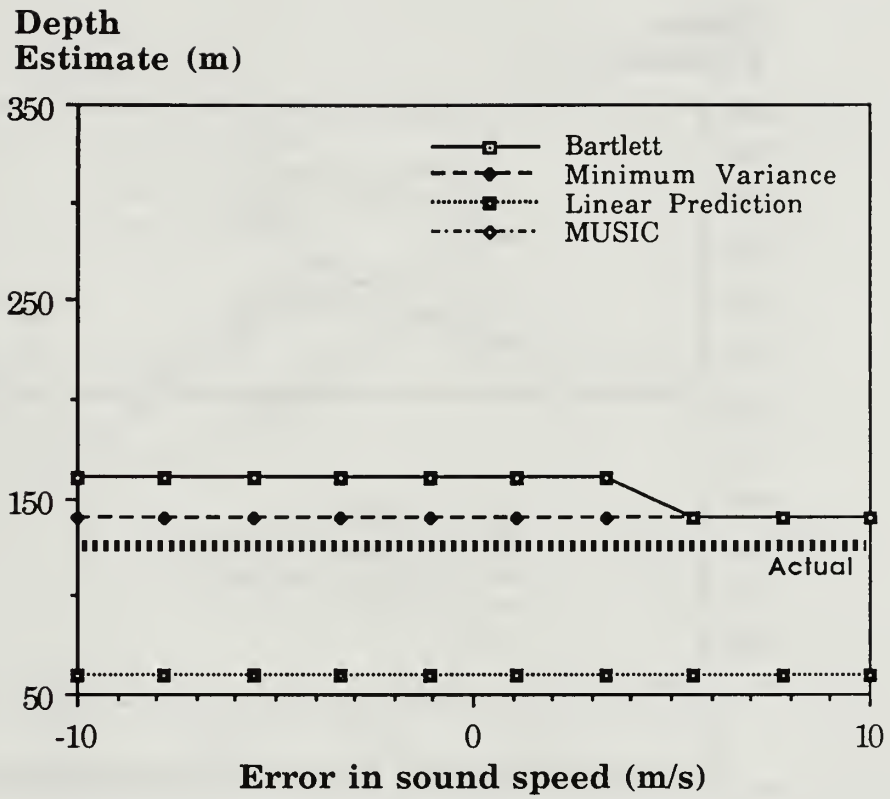

Figure 4.19: Sensitivity to systematic error in SSP (SNR=+10dB, ρ=0.5)

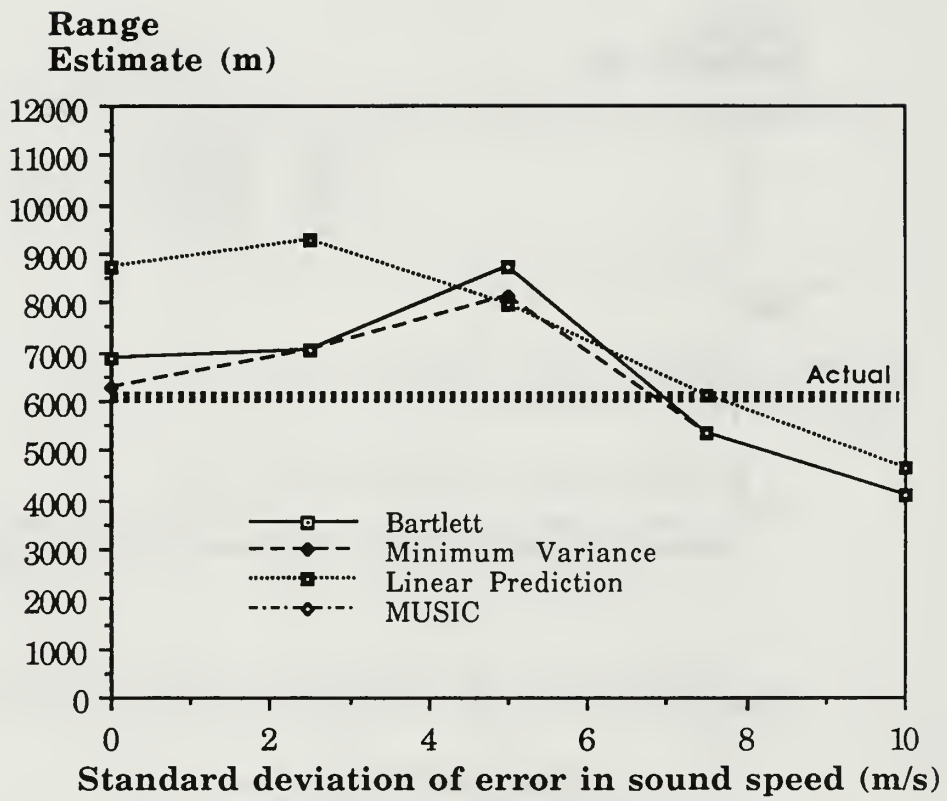

Figure 4.20: Sensitivity to random error in SSP (SNR=+10dB, ρ=0.5)

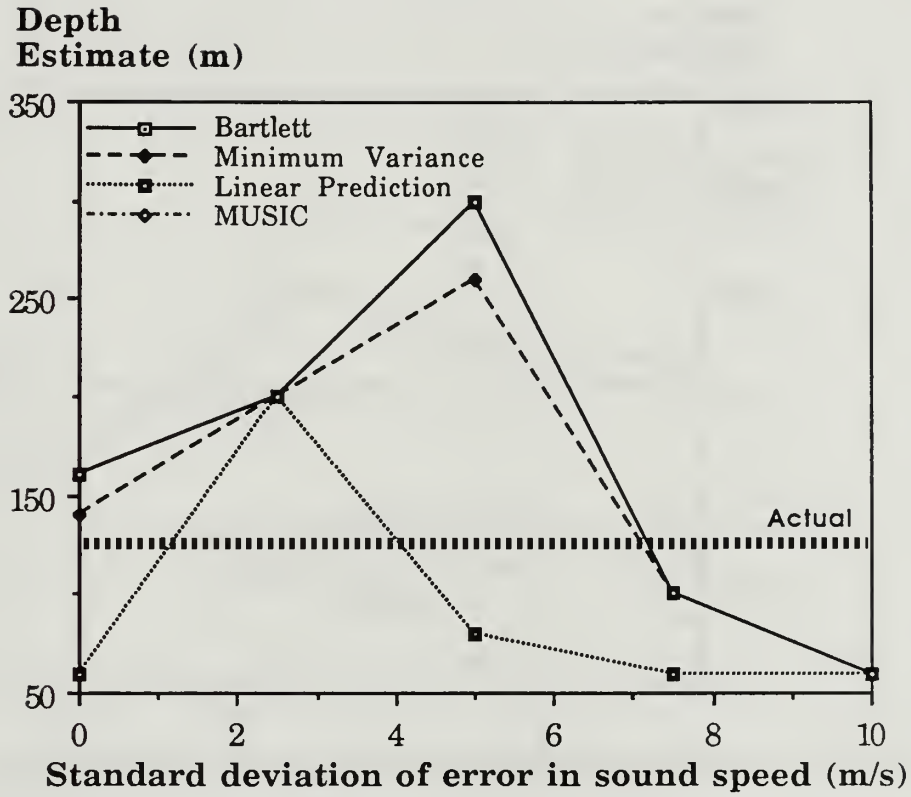

Figure 4.21: Sensitivity to random error in SSP (SNR=+10dB, ρ=0.5)

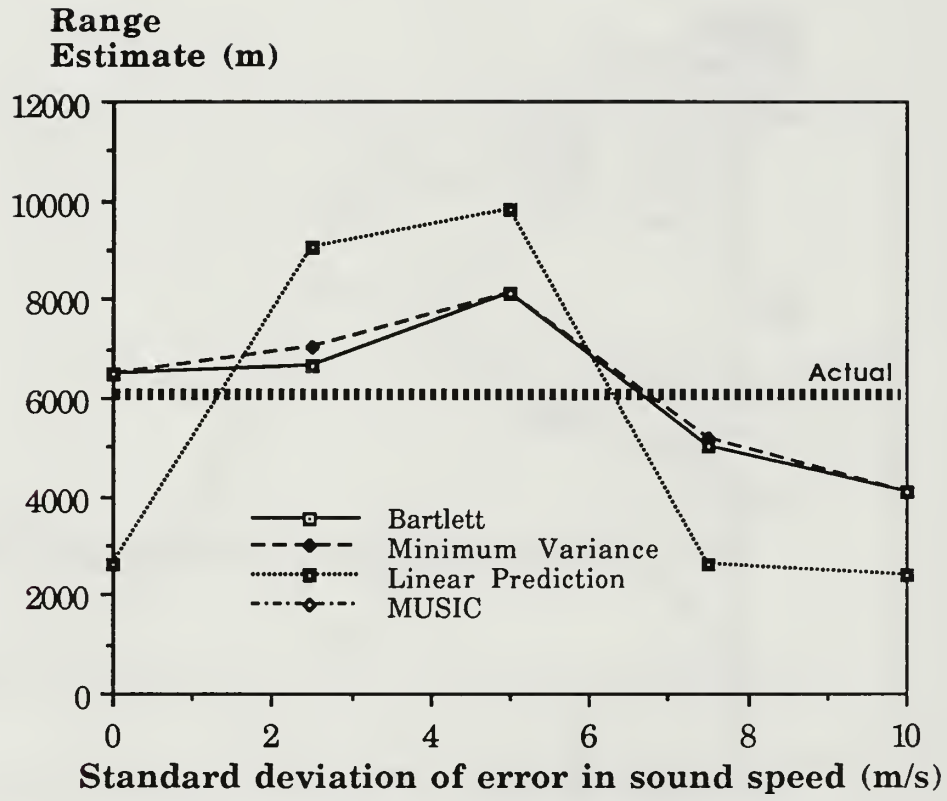

Figure 4.22: Sensitivity to random error in SSP (SNR=+10dB, ρ=0)

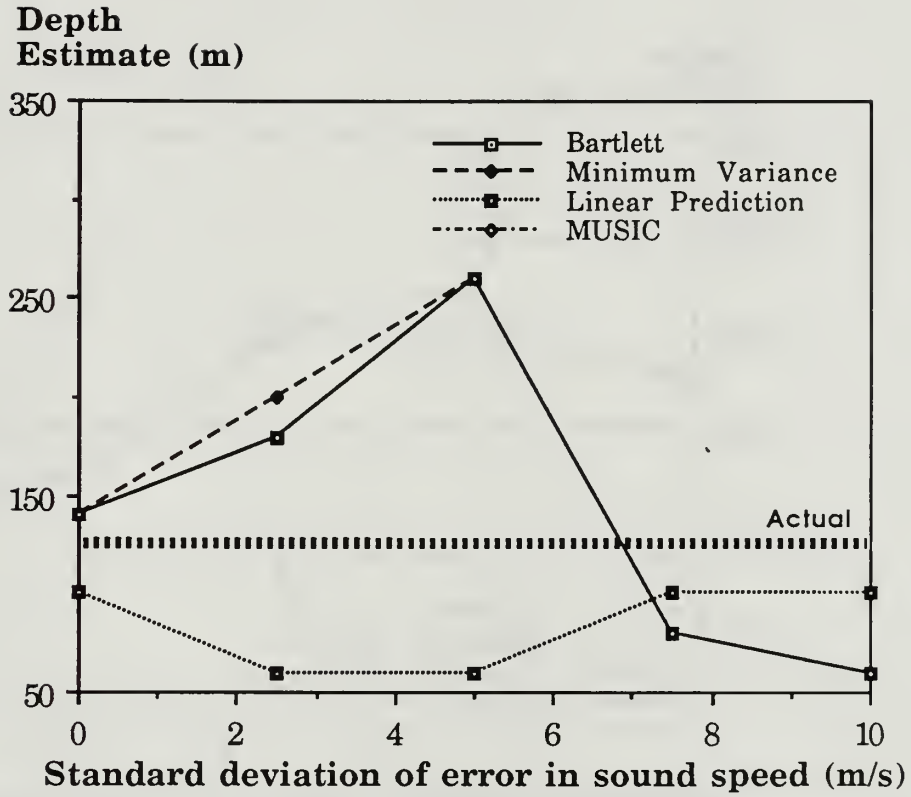

Figure 4.23: Sensitivity to Random Error in SSP, SNR=+10 dB, ρ=0

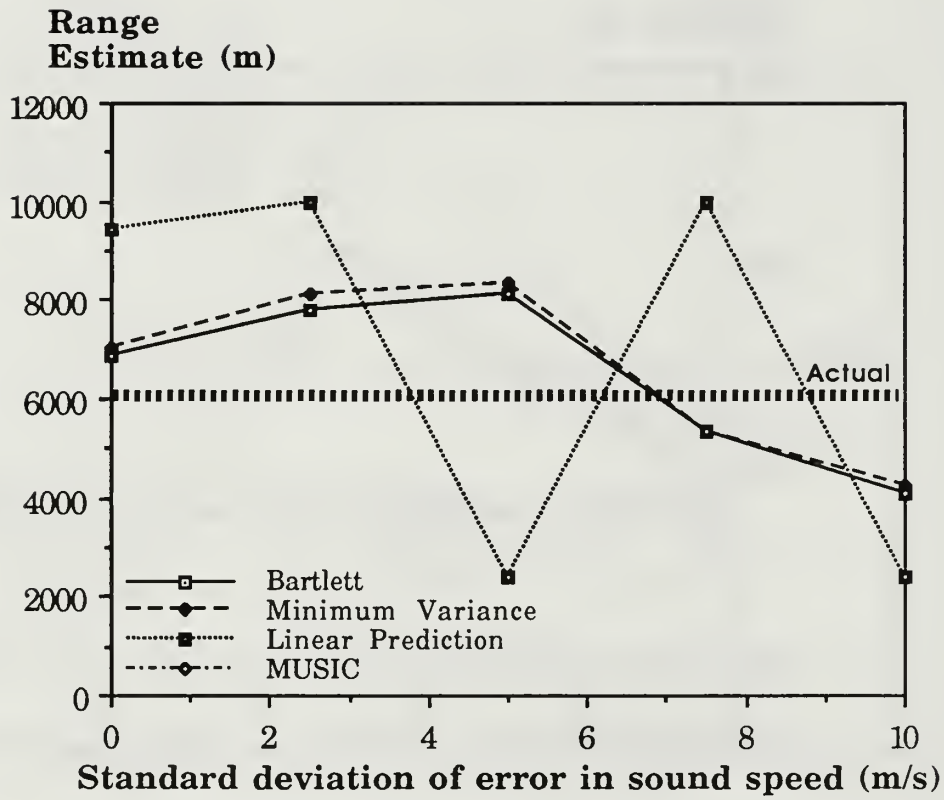

Figure 4.24: Sensitivity to random error in SSP (SNR=0dB, ρ=0)

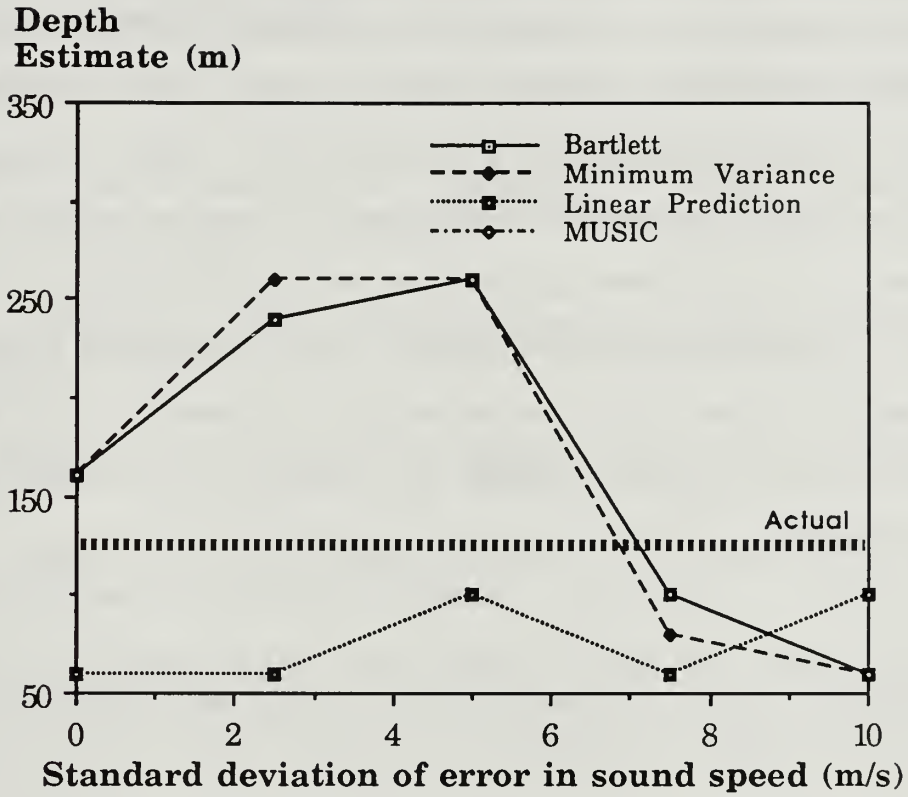

Figure 4.25: Sensitivity to Random Error in SSP, SNR=0 dB, ρ=0

V. CONCLUSIONS AND RECOMMENDATIONS

Based on our research, the behavior of the Bartlett, Minimum-Variance, Linear Prediction, and MUSIC methods in the context of MFP is entirely analogous to their behavior in the context of PWB. In particular, the MUSIC method exhibits higher resolution and greater resistance to noise than the other three methods. Furthermore, the MUSIC method appears to be as robust as the Bartlett and Minimum-Variance methods with respect to errors in the assumed sound speed profile. It is therefore recommended that the MUSIC method be studied further in its MFP application, and compared further with other algorithms, especially in the performance areas of multiple target location and behavior in more realistic acoustic environments.

LIST OF REFERENCES

Baggeroer, A.B., Kuperman, W.A., and Schmidt, H., "Matched field processing: Source localization in correlated noise as an optimum parameter estimation problem," J. Acoust. Soc. Am., v. 83, pp. 571–587, 1988.

Capon, J., "High resolution frequency wave number spectrum analysis", Proc. IEEE, v. 57, pp. 1408–1418, 1969.

Clay, C. S. and Medwin, H., *Acoustical Oceanography*, p. 296, John Wiley & Sons, 1977.

DeGraaf, S.R., and Johnson, D.H., "Capability of Array Processing Algorithms to Estimate Source Bearings," IEEE Trans. Acoust., Speech, Signal Process , v. 33, p. 1368.

Fizell, R.G., "Application of high-resolution processing to range and depth estimation using ambiguity function methods," J. Acoust. Soc. Am., v. 82, pp. 606–613, 1987.

Kay, S. M., Modern Spectral Estimation: Theory & Application, Prentice-Hall, 1988.

Klemm, R., "Range and Depth Estimation by Line Arrays in Shallow Water," Signal Process. v. 3, pp. 333–344, 1981.

Massachusetts Institute of Technology Lincoln Laboratory Project Report TST-72, "Performance Comparison of Superresolution Array Processing Algorithms," A.J. Barabell, J. Capon, D.F. DeLong, K.D. Senne, and J.R. Johnson, 1984.

Naval Postgraduate School Report NPS61-83-002, "An Introduction to the Parabolic Equation for Acoustic Propagation," A. B. Coppens, 1982.

Porter, M.B., and Reiss, E.L., "A numerical method for bottom interacting ocean acoustic normal modes," J. Acoust. Soc. Am., v 77, pp. 1760–1767, 1985.

Roy, R.H., *ESPRIT: Estimation of Signal Parameters via Rotational Invariance Techniques*, PhD Dissertation, Stanford University, 1987.

Schmidt, H. and Glattetre, J., "A fast field model for three-dimensional wave propagation in stratified environments based on the global matrix method," J. Acoust. Soc. Am., v. 78, pp. 2105–2114, 1985.

Schmidt, R. O., *A Signal Subspace Approach to Multiple Emitter Location and Spectral Estimation,* PhD Dissertation, Stanford University, 1981.

Van Veen, B. D. and Buckley, K., "Beamforming: A Versatile Approach to Spatial Filtering," IEEE ASSP Magazine, v. 5, pp. 4–24, 1988.

APPENDIX— A GEOMETRIC APPROACH (SCHMIDT,1981)

PROBLEM

Introduction

Given an array of M sensors (with *arbitrary* locations and response patterns) responding to signals from one or more point sources and noise, we wish to determine the number of signals, their DOA's and their parameters (frequency, amplitude, polarization, etc.). We will assume that sources are in the far field, so that the wavefronts are essentially planar. We also assume that the signals $s(t)$ emitted by the sources of interest are narrowband random processes of the form*

$$s(t) = u(t) \exp(j\omega t).$$

The narrowband assumption means that the modulating function u and the array geometry are such that u is essentially constant over the extent of the array.

Signal Model

Unless otherwise stated, we will assume that we have *deterministic* signals in *additive* white Gaussian noise

$$\mathbf{z}(t) = \sum_{i=1}^{d} \mathbf{a}(\theta_i)\, s_i(t) + \mathbf{n}(t) = \mathbf{x}(t) + \mathbf{n}(t),$$

---

* For convenience, we will deal with the complex pre-envelopes of the signals of interest. Thus, any use of the word "signal" refers to the pre-envelope of a real signal rather than to the signal itself.

where the (normalized) *array response vector* **a** is defined as

$$\mathbf{a}(\theta_i) = [a_1(\theta_i)\, e^{-j\omega_i\tau_1(\theta_i)} \cdots\ a_M(\theta_i)\, e^{-j\omega_i\tau_M(\theta_i)}]^T .$$

$a_k(\theta_i)$ is the output amplitude of sensor k when signal of unit amplitude from DOA θ_i is incident upon it; $\mathbf{x}(t)$, $\mathbf{y}(t)$, and $\mathbf{z}(t)$ are vectors whose components are the signal, noise, and signal-plus-noise, respectively, at the individual sensors; θ_i is the DOA of the ith source (which may be a *vector* parameter with elements such as azimuth and elevation, but will usually refer to the single *scalar* parameter azimuth); ω_i is the center frequency of the signal $s_i(t)$ from the ith source; $\tau_k(\theta_i)$ is the time required for a signal from the ith source to reach the kth sensor; d is the number of signals; M is the number of sensors ($M>d$); and t is time (either continuous or discrete). Note that for the case of a linear array with uniformly spaced elements, $\mathbf{a}(\theta)$ has the same mathematical form as the response of a tapped delay line filter, so that the problem of estimating the frequencies of sinusoidal components of a noisy time series may be considered as a special case of the problem at hand.

We will usually use the shorthand

$$\mathbf{x}(t) = \mathbf{A}\mathbf{s}(t),$$

where we define

$$\mathbf{A} = [\mathbf{a}(\theta_1) \cdots\ \mathbf{a}(\theta_d)] \text{ , and}$$

$$\mathbf{s}(t) = [s_1(t) \cdots\ s_d(t)]^T .$$

Note the difference between this signal model (observation noise but no driving noise) and the model assumed, for example, in Maximum Entropy spectral analysis (driving noise but no observation noise).

GEOMETRICAL BACKGROUND

Signal Subspace

Figure 1 is a geometric illustration of the behavior of the signal vector $\mathbf{x}(t)$ (t is taken to be continuous for the present discussion). The coordinate axes represent the responses of the M sensors (M chosen to be 3 for illustration purposes). The components of the vector $\mathbf{x}$ are the (complex) outputs of the individual sensors and are functions of time. The tip of $\mathbf{x}$ then sweeps out a curve as shown as time progresses.

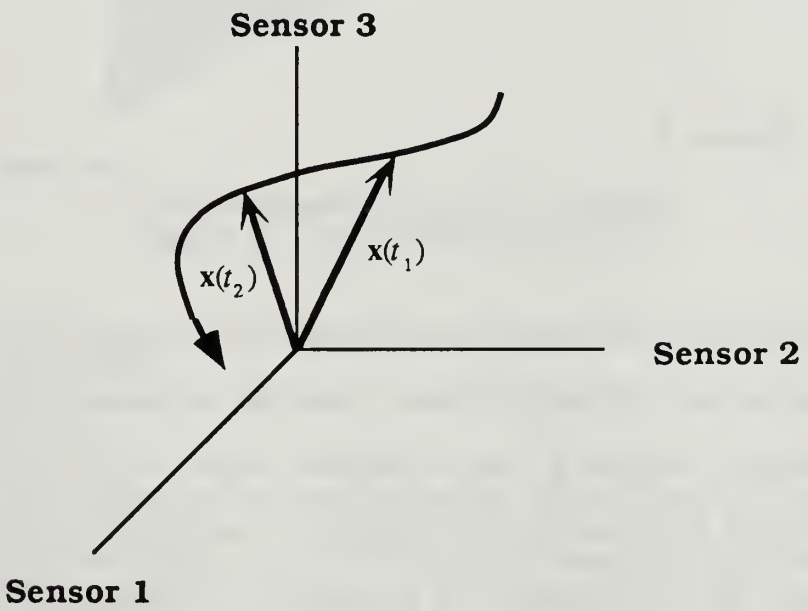

Figure 1: Behavior of signal vector

Consider an example for which d=1 (Figure 2). For this case, as time progresses, each component of $\mathbf{x}$ is multiplied by the *same* time-dependent phase factor. The *magnitude* of $\mathbf{x}$ changes, but its *direction* does not. Therefore, the curve swept out by $\mathbf{x}$ in this case is a *line* passing through the origin.

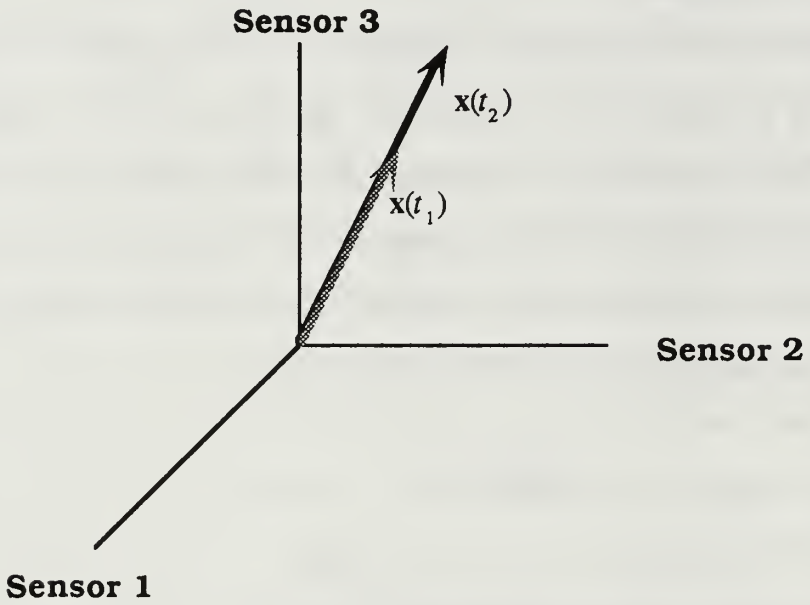

Figure 2: Signal Subspace (d=1)

Consider next an example for the case d=2 (Figure 3). For this case, $\mathbf{x}$ is the vector sum of contributions from the individual signals. These contributions are vectors whose magnitude varies with time, but whose direction is fixed. However, the two vectors are multiplied by *different* time-varying phase factors (because the sources are at different DOA's). Their sum $\mathbf{x}$ therefore sweeps out a curve which is confined to a *plane* passing through the origin.

In general, then, for d sources, the tip of the signal vector $\mathbf{x}$ sweeps out a curve which is confined to a d-dimensional subspace (the *signal subspace*) of $\mathbf{C}^m$. Intuitively, then, we could determine the *number* of emitters by merely measuring the dimension of the signal subspace.

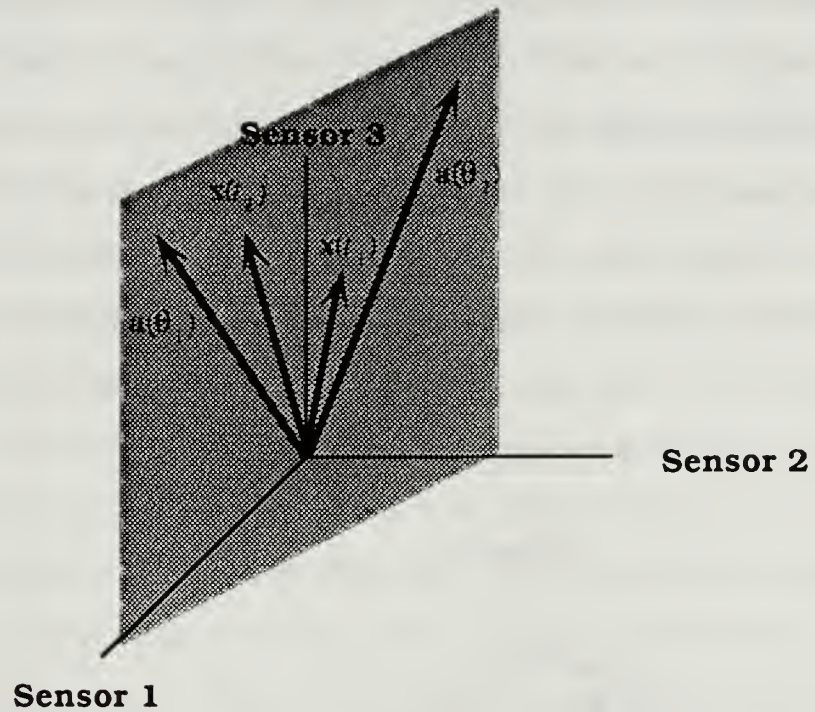

Figure 3: Signal Subspace (d=2)

Array Manifold

Definition

Let $\mathbf{a}(\theta)$ be the (normalized) response of the array to an emitter at DOA θ. We may see (Figure 4) that the tip of $\mathbf{a}$ sweeps out a closed curve (the *array manifold*) in $\mathbf{C}^m$ as θ varies from 0 to 2π. Note that, by definition, $\mathbf{a}$ is independent of time, so that time does not participate in this illustration. It should be noted that, in practice, it is not necessary to have an analytical

expression for $\mathbf{a}(\theta)$: we merely determine it experimentally at a finite number of points, store the results, and recall them as needed (interpolating when necessary).

Ambiguities

It may happen that the array manifold "runs over itself" (*i.e.* the mapping $\mathbf{a}$ from $[0,2\pi]$ into $\mathbb{C}^m$ is not one-to-one). In such a case, the array is said to have an *ambiguity*. Such an ambiguity is not the only kind possible. For example, when the $\mathbf{a}$ vectors corresponding to 3 different DOA's lie in a single plane, the array also has an ambiguity (for reasons that may not be obvious at this point). In general, when the $\mathbf{a}$ vectors corresponding to $n+1$ different DOA's lie in a subspace of dimension n or less, the array is said to have a *rank n* ambiguity.

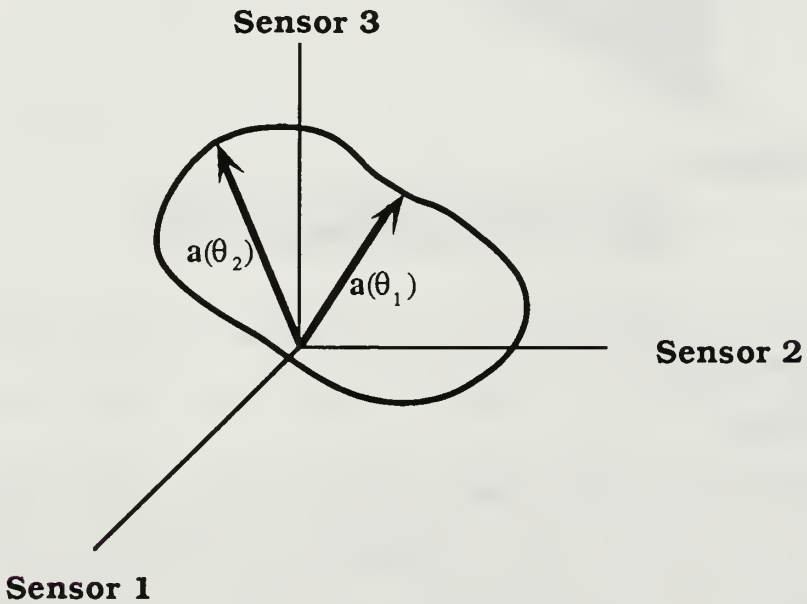

Figure 4: Array manifold

Vector fields

The examples used until now have assumed that the (unnormalized) array response vector for a particular DOA sweeps out a 1-dimensional subspace of $\mathbf{C}^m$ (*i.e.,* a line through the origin). This is not always the case. For example, if the signal of interest is carried by a *vector field* such as electromagnetic radiation, the array may respond differently to different polarizations of the signal. For such a case, the **a** vector sweeps out a 2-dimensional subspace as polarization varies (for a fixed DOA). The array manifold for such a situation might then be visualized as a closed *sheet* rather than a loop. For simplicity, in the sequel we will limit ourselves to the case of *scalar* fields.

DOA Determination

For the case of one emitter, it is clear that the array response **a** corresponding to the source DOA lies in the (1-dimensional) signal subspace. In order to determine the DOA, then, we could merely observe the behavior of the signal vector **x** (if no noise were present) to determine the signal subspace, find the single unit vector that spans the subspace, and invert the mapping **a** (which is one-to-one unless the array has an ambiguity) to determine the DOA.

For the case of two emitters, recall that the signal vector **x** is the sum of (vector) contributions from the individual emitters. Obviously, these contributions are merely scalar multiples of the **a** vectors corresponding to the two emitter DOA's. We see, then, that the signal subspace is spanned by these two **a** vectors. If the array has no ambiguities, there is no third **a**

vector that lies in the subspace. Thus, just as in the case of one emitter, we may invert the **a** mapping to determine the DOA's (Figure 5).

In general, we observe the data vector **x**, determine the signal subspace, find its intersection (*d* different **a** vectors) with the array manifold, and invert the mapping $\mathbf{a}(\theta)$ to obtain the DOA's. Ambiguities would obviously prevent such an inversion, but they may be avoided by proper array design (although sometimes physical constraints, such as in towed sonar arrays, preclude such design).

Multipath

It is possible for the emissions from a single source to arrive by two or more different paths (*e.g.*, as a result of reflection from the ocean surface, in the case of underwater acoustics). As an illustration, consider the case of an array receiving signals from one emitter via two different DOA's. In such a case, the two signals will exhibit perfect temporal correlation (at least in theory). Recall that it is the *independent* variation with time of the array output due to individual signals from different DOA's that causes the the signal vector to sweep out a two-dimensional subspace (Figure 3). In the multipath case, however, the array no longer responds *independently* to signals received from the two DOA's: the signal subspace is *one-dimensional* (Figure 5). In addition, note that this signal subspace is *not* spanned by any combination of vectors in the array manifold. Evidently, this geometric approach is incapable of dealing with *perfectly coherent* multipath. However, such multipath is rarely, if ever, observed in real life.

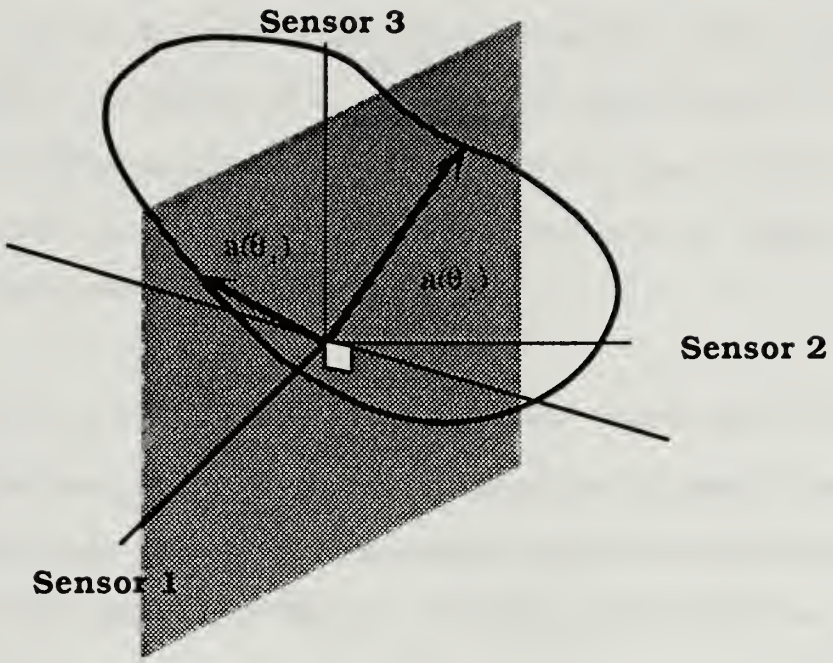

Figure 5: DOA Determination

Noise

The above discussion assumes that no noise is present. The simple techniques described are clearly not valid if it *is* present. Because of noise, the signal+noise vector **z** sweeps out a curve that no longer lies in the signal subspace. Also, as a result of measurement and estimation errors, what would (in the noiseless case) be intersections between the array manifold and the signal subspace become "near misses" when noise is present.

Essentially, the previously mentioned technique is modified as follows. Recalling the assumed form for the data model, we see that

$$\mathbf{R}_{zz} = \mathbf{ASA}^H + \sigma^2 \Sigma_n ,$$

where we define

$$\mathbf{R}_{zz} = E[\mathbf{z}\mathbf{z}^H],$$

$$\mathbf{S} = \mathbf{s}\mathbf{s}^H, \text{ and}$$

$$\sigma^2 \Sigma_n = E[\mathbf{n}\mathbf{n}^H].$$

(we normalize the noise covariance so that trace $\Sigma_n = m$). All of these autocorrelation matrices are assumed to be *theoretical*, not *estimated*. It may be shown that the array response vectors **a** are *not* eigenvectors of the matrix $\mathbf{R}_{zz}$, so that we must consider the generalized eigenvalue problem

$$\begin{aligned} 0 &= \det[\mathbf{R}_{zz} - \lambda \Sigma_n] \\ &= \det[\mathbf{A}\mathbf{S}\mathbf{A}^H + \sigma^2 \Sigma_n - \lambda \Sigma_n] \\ &= \det[\mathbf{A}\mathbf{S}\mathbf{A}^H - (\lambda - \sigma^2)\Sigma_n] \\ &= \left\{\det\left[\Sigma_n^{\frac{-1}{2}} \mathbf{A}\mathbf{S}\mathbf{A}^H \Sigma_n^{\frac{-H}{2}} - (\lambda - \sigma^2)\mathbf{I}\right]\right\}\left\{\det \Sigma_n\right\}, \end{aligned} \quad (1)$$

so that the *generalized* eigenvalue problem has been transformed into an *ordinary* one. The positive-definite square root $\Sigma_n^{\frac{1}{2}}$ of Σ_n is defined as

$$\Sigma_n^{\frac{1}{2}} = \mathbf{E}_\Sigma \Lambda_\Sigma^{\frac{1}{2}} \mathbf{E}_\Sigma^H,$$

where $\mathbf{E}_\Sigma$ is the matrix whose columns are the (ordinary) eigenvectors of Σ_n, and $\Lambda_\Sigma^{\frac{1}{2}}$ is the diagonal matrix whose elements are the square roots of the (ordinary) eigenvalues of Σ_n , arranged in decreasing order. It may be seen that the first term in equation (1) is an $m \times m$ matrix of rank d. That term therefore has d non-zero eigenvalues and $m-d$ zero eigenvalues. So, the set $\{\lambda_i\}$ of eigenvalues is of the form

$$\{\lambda_i\} = \{\nu_1 + \sigma^2, \cdots \nu_d + \sigma^2, \sigma^2 \cdots \sigma^2\} .$$

The m eigenvectors form an orthogonal set. It may be shown that the eigenvectors corresponding to the d principal (*i.e.,* not repeated) eigenvalues span the same subspace as the signal vectors $\mathbf{x}$. In the presence of noise, then, the signal subspace may be determined by solving a generalized eigenvalue problem. The $m-d$ remaining eigenvectors span the *noise subspace* (the orthogonal complement to the signal subspace).

In practical applications, the autocorrelation matrices are never known exactly, but must be estimated from the observations. Because of estimation errors, the noise eigenvalues (*i.e.,* the lowest $m-d$ eigenvalues) will not be exactly equal, so that even the number of emitters d cannot be estimated with certainty. For the purpose of the present discussion, however, we assume that d is known. Optimal estimates of the signal subspace may then be obtained via the standard Linear Least Squares, Maximum Likelihood, or Maximum Entropy techniques. All three techniques give the same result, but one which is computationally infeasible in practice. The following suboptimal algorithm arose out of the need for lower computational requirements.

THE MUSIC ALGORITHM

Estimating the Subspace Dimension

In an *optimal* estimator, the problem of estimating the subspace dimension cannot be decoupled from that of estimating the subspace itself. However, in the interest of reducing computational load, we will determine the dimension (number of emitters) separately. This feature of the MUSIC algorithm therefore causes it to be suboptimal. Essentially, to determine the number of emitters, we perform a generalized eigendecomposition of the signal-plus-noise covariance matrix and then take the estimated number of emitters to be the number of generalized eigenvalues exceeding some threshold (recall that, in theory, for d sources and m receivers, there will be $m-d$ generalized eigenvalues equal to the noise power).

Estimating the Signal Parameters

In the presence of noise, we can no longer depend on precise intersections between the signal subspace and the array response vectors corresponding to the signal DOA's. To estimate these DOA's, we must therefore determine those **a** vectors which are "closest" (in some sense) to the signal subspace. The algorithm discussed in the following is known as conventional or *Spectral* MUSIC and is one possible method for doing this.

Recall from the earlier discussion that for the noiseless case, the array response vectors corresponding to the signal DOA's are orthogonal to the noise subspace. The squared length l^2 of the projection of an **a** vector onto the noise subspace is given by

$$l^2(\theta) = \mathbf{a}^H(\theta)\mathbf{E}_N\mathbf{E}_N^H\mathbf{a}(\theta)\,.$$

In the presence of noise, however, l^2 will generally not be zero for any **a**. We must therefore search the array manifold for the set of d array response vectors which result in the lowest value for the quantity. An alternative method for accomplishing this is to define the "spectrum"

$$P_M(\theta) = \frac{1}{\mathbf{a}^H(\theta)\mathbf{E}_N\mathbf{E}_N^H\mathbf{a}(\theta)}.$$

The angles corresponding to the peaks of this "spectrum" are taken as the estimated DOA's. The word "spectrum" appears in quotes because, although the function is similar in some respects to power spectral density functions, the peak heights do not necessarily provide any information about the power in their respective components.

Modifications of the basic MUSIC technique are possible and are superior in certain situations, but will not be discussed here (see *e.g.*, DeGraaf and Johnson, 1985).

INITIAL DISTRIBUTION LIST

	No. Copies
1. Defense Technical Information Center Cameron Station Alexandria, VA 22304-6145	2
2. Library, Code 0142 Naval Postgraduate School Monterey, CA 93943-5002	2
3. Prof. C.W. Therrien, Code 62Ti Naval Postgraduate School Monterey, CA 93943	6
4. Prof. J.H. Miller, Code 62Mr Naval Postgraduate School Monterey, CA 93943	1
5. Prof. R. Hippenstiel, Code 62Hi Naval Postgraduate School Monterey, CA 93943	1
6. Dr. R. Madan ONR Code 1114 Arlington, VA 22217-5000	1
7. ECE Department, Code 62 Naval Postgraduate School Monterey, CA 93943	1
8. LT D.D. Pierce 437 E. Fairmount Ave. State College, PA 16801	3

612-587

Thesis
P5331 Pierce
c.1 Matched field processing for underwater source location.

Thesis
P5331 Pierce
c.1 Matched field processing for underwater source location.

AMERICAN BINDERY TOPEKA KANSAS

Matched field processing for underwater
3 2768 000 88118 9
DUDLEY KNOX LIBRARY